CHALMERS
UNIVERSITY OF TECHNOLOGY

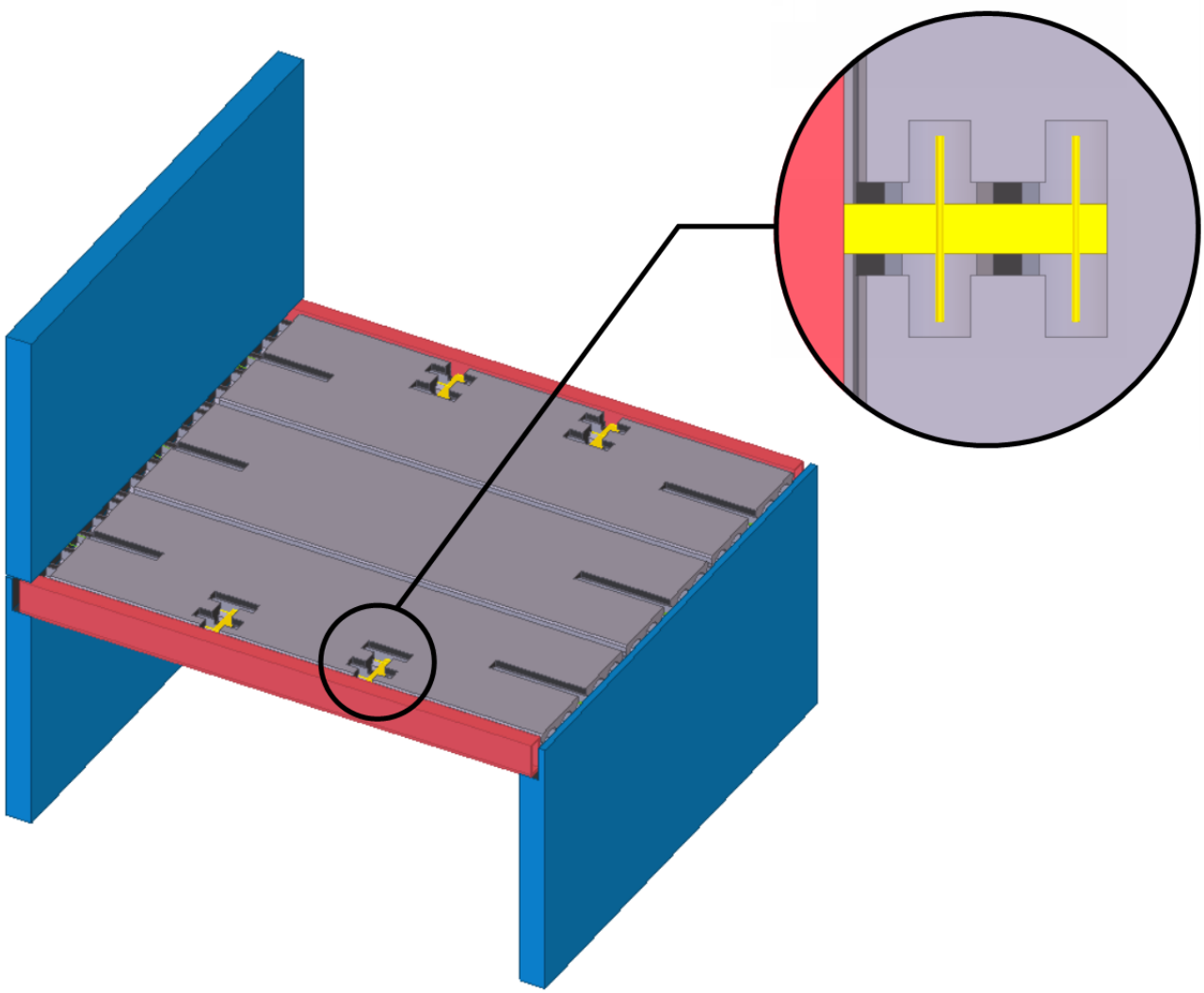

Transverse Connection to Hollow Core Units

An Experimental Study Concerning In-Plane Shear Forces

Master's thesis in the Master's programme Structural Engineering and Building Technology

ALEXANDRA ERIKSEN & EMMA HEDIN

Department of Architecture and Civil Engineering
Division of Structural Engineering
Concrete Structures
CHALMERS UNIVERSITY OF TECHNOLOGY
Master's Thesis ACEX30-18-9
Gothenburg, Sweden 2018

MASTER'S THESIS ACEX30-18-9

Transverse Connection to Hollow Core Units

An Experimental Study Concerning In-plane Shear Forces

Master's Thesis in the Master's Programme Structural Engineering and Building Technology

ALEXANDRA ERIKSEN
EMMA HEDIN

Department of Architecture and Civil Engineering
Division of Structural Engineering
Concrete Structures
CHALMERS UNIVERSITY OF TECHNOLOGY
Göteborg, Sweden 2018

Transverse Connection to Hollow Core Units
An Experimental Study Concerning In-plane Shear Forces

Master's Thesis in the Master's Programme Structural Engineering and Building Technology

ALEXANDRA ERIKSEN

EMMA HEDIN

Examensarbete ACEX30-18-9
Institutionen för arkitektur och samhällsbyggnadsteknik
Chalmers tekniska högskola, 2018

Department of Architecture and Civil Engineering
Division of Structural Engineering
Concrete Structures
Chalmers University of Technology
SE-412 96 Göteborg
Sweden
Telephone: + 46 (0)31-772 1000

Cover:
A prefabricated structure showing location of the studied connection, together with a detail section of the steel component KBA-5 which is a part of the connection.

Chalmers reproservice / Department of Architecture and Civil Engineering
Göteborg, Sweden, 2018

Transverse Connection to Hollow Core Units

An Experimental Study Concerning In-plane Shear Forces

Master's thesis in the Master's Programme Structural Engineering and Building Technology

ALEXANDRA ERIKSEN

EMMA HEDIN

Department of Architecture and Civil Engineering
Division of Structural Engineering
Concrete Structures
Chalmers University of Technology

ABSTRACT

In prefabricated structures, connections constitute as vital parts as they transfer forces between the individual prefabricated elements, and thus allows the structure to act as one complete unit. Floor systems, composed by hollow core units, in such a structure, contribute to the overall stiffness, mainly by diaphragm action and lateral stability. The most critical section, regarding horizontal forces, is located at the outermost edge of the floor system, where the shear force is of maximum magnitude.

The aim of the study was to understand the structural behaviour and be able to quantify the load-carrying capacity, of a connection located at the most critical section in a floor system, when loaded laterally in-plane. The connection investigated in this study includes a transverse, hidden steel component with the commercial name KBA-5. To achieve the aim, structural tests of a designed test arrangement were performed. Further, an analytical model, based on the strut and tie method of the designed test arrangement, was developed. The maximum experimental failure load and structural behaviour in the analytical model were further compared to the structural tests.

The designed test arrangement was composed of a symmetrical system of two hollow core units, attached to a steel beam through the steel component KBA-5. The main limitation of the test setup was the test machine which in turn limited the length of the hollow core units to 800 mm. This generated concentrated stress fields; to study the effect of these, two different support locations were tested, which respectively gave an average experimental failure load of 200 kN and 95 kN.

The analytical model was developed for tests with support location at second web, and showed good correlation to the structural tests, in terms of loading paths corresponding to crack patterns found in the structural tests. The calculated failure load was 59 kN, to be compared with the experimental value of 200 kN, thus corresponding to 30 % of the average experimental failure load.

Finally, it was difficult to determine how well the performed structural tests corresponded to reality. The major reasons for differences were the stress fields, which in real structures are not as concentrated as in the structural tests. However, the analytical model reflected the behaviour of the structural tests in a good manner.

Key words: Prefabricated, connection, hollow core units, in-plane shear force, structural tests, structural behaviour, load-carrying capacity, strut and tie method

Transversell koppling till håldäckselement

En experimentell studie gällande skjuvkrafter i planet

Examensarbete inom masterprogrammet Structural Engineering and Building Technology

ALEXANDRA ERIKSEN

EMMA HEDIN

Institutionen för arkitektur och samhällsbyggnadsteknik
Avdelningen för Konstruktionsteknik
Betongbyggnad
Chalmers tekniska högskola

SAMMANFATTNING

Kopplingar i prefabricerade stommar har en viktig roll då de överför laster mellan individuella prefabricerade element och får stommen att bete sig som en enhet. I prefabricerade stommar bidrar golvsystem, av håldäckselement, till den övergripande och den laterala stabiliteten. Den avgörande sektionen, avseende horisontella krafter, är lokaliserad vid den yttre kanten av golvsystemet där skjuvkraften är störst.

Syftet med studien var att förstå det strukturella beteendet och kvantifiera kapaciteten för en koppling belägen i den mest kritiska sektionen i ett golvsystem, när den är lateralt belastad i planet. Kopplingen som undersöktes i denna studie innehöll en transversell, dold stålkomponent med det kommersiella namnet KBA-5. Försök genomfördes, där provkroppar belastades till brott i en utformad provuppställning. Vidare utvecklades en analytisk modell, baserad på en fackverksmetod, av provuppställningen. Den experimentella maximala brottlasten och det strukturella beteendet jämfördes mellan den analytiska modellen och belastningsförsöken.

Den valda provuppställningen var symmetrisk, bestående av två håldäckselement fastsatta mot en stålbalk genom stålkomponenten KBA-5. Provningsmaskinen var en huvudsaklig begränsning, vilken begränsade längden av håldäcken till 800 mm, vilket i sin tur genererade i ett koncentrerat spänningsfält. För att se hur detta påverkade försöken, utfördes provningarna med två olika stödplaceringar. Den experimentella brottlasten för de olika stödpositionerna var 200 kN och 95 kN.

Den analytiska modellen utvecklades för försök med stöd vid andra livet och fungerade väl som förklaringsmodell för kraftspelet i försöken, då provkropparnas sprickmönster kunde identifieras och förklaras. Den beräknade brottslasten var 59 kN, att jämföra med experimentell last om 200 kN, dvs motsvarande 30 % av den experimentella brottlasten.

Slutsatsen av studien var att det fanns svårigheter i att bestämma hur väl de genomförda belastningsproverna motsvarade verkligheten. Detta då spänningsfälten var mer koncentrerade i de genomförda försöken än vad som är fallet i en verklig stomme. Däremot reflekterade den analytiska fackverksmodellen det strukturella beteendet för belastningsproven på ett bra sätt.

Nyckelord: Prefabricerad, koppling, håldäckselement, skjuvkrafter i planet, belastningsprov, strukturellt beteende, kapacitet, fackverksmetod.

Contents

Preface

The study has been carried out from January 2018 to June 2018. In this study, a structural test on a transverse connection in hollow core units has been performed. The study has been carried out at the Division of Structural Engineering, Concrete Structures, Chalmers University of Technology, Sweden, together with the company Kynningsrud Prefab AB. The structural tests have been performed at the factory of Kynningsrud Prefab AB in Uddevalla, Sweden.

Examiner of the study has been Professor Karin Lundgren and supervisor of the study was M.Sc. Per-Arne Andersson from the company Kynningsrud Prefab AB.

We would like to thank the staff at Kynningsrud Prefab AB for co-operation and involvement in the structural test, and a special thanks to Christian Larsson and Christoffer Hjortskog for assistance during the structural tests. Thank you, Research Engineer Sebastian Almfeldt, for lending us the measurement devices. We also would like to thank our examiner Lundgren and supervisor Andersson for their engagement and support through the difficulties during the study.

We also would like to give a special thanks to Professor Björn Engström, for his engagement and time to help us with the strut and tie models.

Finally, a huge thanks to our families and friends for your invaluable support during our five years of studies.

Göteborg June 2018

Alexandra Eriksen & Emma Hedin

Notations

Abbreviations

2D	Two-dimensional
3D	Three-dimensional
BC	Boundary condition
FEA	Finite element analysis
HC	Hollow core
KPAB	Kynningsrud Prefab AB

Roman upper case letters

A_{c0}	Loaded area
A_{c0A}	Loaded area A_{c0} from section A
A_{c0B}	Loaded area A_{c0} from section B
A_{c1}	The maximum distribution area with the same shape as A_{c0}
A_i	Loaded joint area
A_s	Steel area crossing a joint
F_{Rdu}	Capacity for local crushing
S_{Ed}	Designing tensile force
$S_{Rd.c}$	Maximum tensile capacity

Roman lower case letters

a	Penetration length in concrete of a component
b_1	Width of loaded area
b_2	Width of the maximum distribution area
c	Parameter affected by roughness of interfaces
d_1	Length of loaded area
d_2	Length of the maximum distribution area
f_{cd}	Design strength of concrete
f_{ck}	Characteristic compressive cylinder strength of concrete, at 28 days
f_{cm}	Average value of concrete cylinder compressive strength
$f_{cm.cube}$	Average compressive strength of concrete from cube test
f_{ctd}	Design tensile strength of concrete
f_{yd}	Design yield strength of steel

s	Minimum centre distance between two components
s_{dU}	Upper limit design value of tensile strength
s_{Rd}	Required centre distance between components
t_{min}	Thickness of the thinnest layer of concrete
v_{Rdi}	Shear stress capacity

Greek letters

α	Angle of how a component crosses a joint
γ	Partial factor for concrete
μ	Parameter affected by roughness of interfaces
ν	Strength reduction factor
ρ	Factor dependent on areas affecting a joint
σ_n	Normal stress

1 Introduction

As a finalised structure, a cast in situ building and a prefabricated structure will look similar, but their behaviour of handling loads, and other actions differ. The prefabricated structure cannot be seen as a cast in situ structure divided into smaller parts, since it is designed and constructed based on other characteristics and prescriptions. Unlike a continuous cast in situ structure, a full working prefabricated structural system requires adequate connections between individual neighbouring elements to get a good performance. The purpose of the connections is to transfer forces between the elements and eventually to the foundation (Fib, 2008).

Prefabricated structures are connected in a mechanical way, and examples of components used in such connections are bolts, reinforcing steel and welds. The grout in the cavities between the elements are also a common way to transfer forces between the prefabricated units, and by using different components combined with the grouting, the structural integrity of the structure is strengthened. To choose what connection should be used, what component should be included and where it is appropriate to apply, it is important to understand the flow of forces in both vertical and horizontal direction. By this understanding, the intended structural behaviour can be determined and the choice of what connection should be used becomes easier (Fib, 2008).

To achieve stability of a prefabricated structure, various types of systems can be used. One common system is floor systems which can consist of different types of units, e.g. hollow core (HC) units which are a part in this study. The floor systems contribute to the overall stiffness of the structure, mainly by diaphragm action and transverse distribution of forces. The diaphragm action transfer in-plane shear forces between HC units and between the units and surrounding structural members. The maximum value of the shear force, and thus the most critical section, can be found on the outermost edge of the floor system where the shear force eventually ends. Therefore, substantial connections at this location, are needed to transfer these forces into neighbouring elements and to ensure diaphragm action (Fib, 2014).

The connection investigated in this study, is located on the longitudinal edge of a HC unit. This connection is used to resist, and transfer, in-plane shear forces and includes the component with the commercial name KBA-5. It is a transverse, hidden, component, which is assembled by a steel plate and two reinforcement bars welded to the plate. The component is placed inside the HC units on site in a premade recess, and each reinforcement bar is placed in one void respectively. The end of the component is welded directly to a steel beam. The location of the connection including multiple numbers of the component KBA-5, together with a close up of the component KBA-5, can be seen in Figure 1.1.

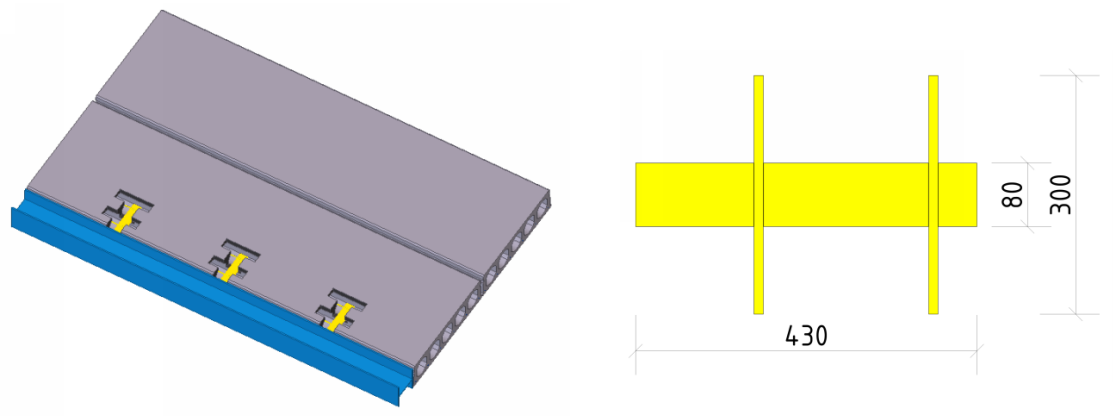

Figure 1.1 The location of the studied component at the longitudinal edge of the hollow core units, and a close up of the steel component KBA-5 with dimensions in mm.

The capacity of the studied connection is today theoretically calculated based on EN-1992-1-1 (2008a), EN-1993-1-1 (2008b) and EN-1993-1-8 (2008c) and the Norwegian handbook Betongelementboken (2013). These calculations are based on separate failure modes but do not take the complete structural behaviour into account.

1.1 Aim and objectives

The aim of this study is to understand the structural behaviour and be able to quantify the load-carrying capacity of the connection including the component KBA-5, when loaded laterally in-plane.

To achieve this aim, the following objectives need to be met:

- Analyse floor systems, consisting of hollow core units, to understand the need for load-carrying capacity of the connection.
- Develop a suitable test arrangement to reflect the structural behaviour of the studied connection.
- Perform structural tests using the designed test arrangement to measure the experimental structural behaviour and the maximum capacity of the connection.
- Set up analytical calculation methods describing the structural behaviour in the tests and compare the experimental and analytical results.

1.2 Scope and limitations

This study focuses on the effects of in-plane lateral forces acting on a connection located at the longitudinal edge of a HC unit. In this study, the effect of vertical forces is dismissed. Shrinkage, creep and temperature changes are not considered. The weld between the steel beam and the component KBA-5 is assumed to be sufficient, and a possible failure mode concerning the weld is assumed to be negligible.

The available test machine, provided by Kynningsrud Prefab AB, had a limited free height and the load could only be applied vertically, which must be considered when the test specimen was developed. Limitations regarding the test machine are further described in Chapter 6.1.

1.3 Method

To reach the aim and objectives, the implementation of the study is divided into different steps. These are explained below and visualized in Figure 1.2

(i) By a literature review, gain knowledge of the structural response of prefabricated structures, with focus on the response of floor systems containing hollow core units and adequate connections.

(ii) Evaluate both factors affecting the structural test, and possible analytical models.

(iii) Design a test arrangement and perform structural tests, and accomplish suitable analytical models corresponding to the studied case.

(iv) Compare the results from the analytical methods and the structural tests.

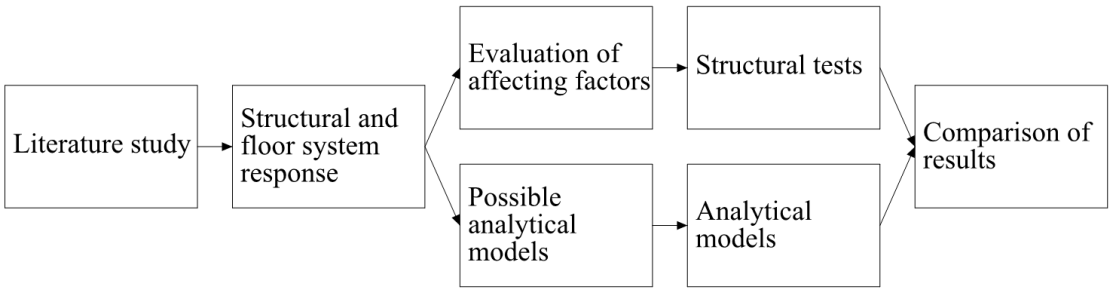

Figure 1.2 Method of study.

2 Prefabricated Structures

Prefabricated structures are composed of several elements, such as columns, walls, beams and floor elements. These elements are then transported to a building site where they later on are mounted together by connections (Fib, 2008). Thus, the connections are the most important factors for prefabricated structures since the purpose of these is to transfer forces through adjacent structural elements and to provide stability (Elliot, 2002). Some of the main advantages with prefabricated concrete structures compared to cast in situ structures are the fast erection time, possibility of long spans, shallow depths of construction floors and the use of high quality concrete (Fib, 2014).

When designing a prefabricated structural system, it is important to have its philosophy of design in mind and remember that it differs from cast in situ structures. Cast in situ structures act as three dimensional (3D) structural frameworks where the connections between the different members, such as floors and walls, are designed to have an equal resistance to loads (Elliott & Jolly, 2013). In contrast, a fundamental requirement for prefabricated structures is to design a load path for every point in the structure, down to the foundation (PCI, 1998). The ability of redistributing forces in cast in situ is greater than in prefabricated structures and due to the lower possibility of force redistribution in the latter structure, design of details such as connections are of greater importance. Thus, the design of prefabricated structural systems consider the overall stability of the structure with respect to both vertical and horizontal forces, the capacity of the prefabricated elements as individual units and also the connections that are used in order to create a full working system (Fib, 2014).

Due to the amount of different structural members that can be used in prefabricated concrete structures, there are several ways structural systems members can be composed in order to achieve stability. The basic types of systems are portal and skeletal, cell, floor and roof, bearing wall and facade systems. They carry loads and actions in different ways, however it is common to use combinations of different precast structural systems. The most appropriate combination of a system is up to the responsible designer (Fib, 2008).

To achieve structural stability of a prefabricated structure there are two main concepts that are used, braced and unbraced structures. The two types of structures carry vertical loads in similar ways but differs in the way of taking care of horizontal forces (Elliott & Jolly, 2013). Unbraced systems are used for structures with a low number of storeys and together with lightweight roofs the horizontal forces are resisted by columns acting as cantilevers. Multi-storey structures are commonly braced structures where e.g. stabilizing walls as lift shafts, internal shear walls or stairwells are used as stabilizing, vertical units. Another option to provide a multi-storey prefabricated structure with an increased lateral and overall stability, a floor system, consisting of HC units, is useful. The main purpose of such a system is to carry vertical loads, but can advantageously be used to transmit horizontal forces, e.g. from wind or earth pressure, acting on the facades or walls underground, into stabilizing vertical members (Fib, 2014).

2.1 Hollow core units

Hollow core units are pretensioned, one-way spanning concrete units, most commonly used as parts of floor and roof systems (PCI, 1998). The standard width of the units is 1200 mm and the most common floor depths in Sweden are between 185 mm and 500 mm (Svensk Betong, 2018). The length of each unit is mainly dependent on what type and magnitude of loading it is exposed to, but regarding the low self-weight compared to length of the units and the pretensioning, long spans are possible. The low weight/length ratio is achieved due to the longitudinal voids the units are provided with, these are of quadratic, rectangular or circular shape (Kynningsrud, 2018). The number of voids in the units are standardized, from six voids in the smallest dimensions to four voids in the largest units (Svensk Betong, 2018). In Figure 2.1 a picture of a HC unit with five voids can be seen.

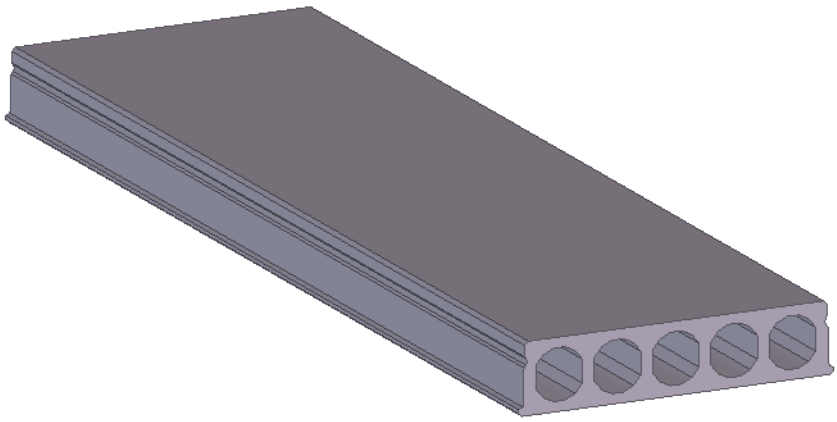

Figure 2.1 A hollow core unit with five voids, in 3D.

The voids in a HC unit results in a cross-section reminding of I-sections, where the concrete between the voids act as webs and the concrete above and below can be seen as flanges (PCI, 1998). The voids and the pretensioning steel wires can be seen in Figure 2.2, where it also can be seen that the outer geometry of the HC unit is not completely rectangular. The HC units used in this study are produced by an extruding machine which makes the longitudinal edge of the units inclined. Due to the extrusion and that the units are produced with a concrete of low slump, the longitudinal edges get surfaces with a slight roughness. The inclination of the edges also simplifies the possibility of filling the joints between the HC units with grout and together with the roughness, this increases the ability of transferring forces between the units (Elliot, 2002).

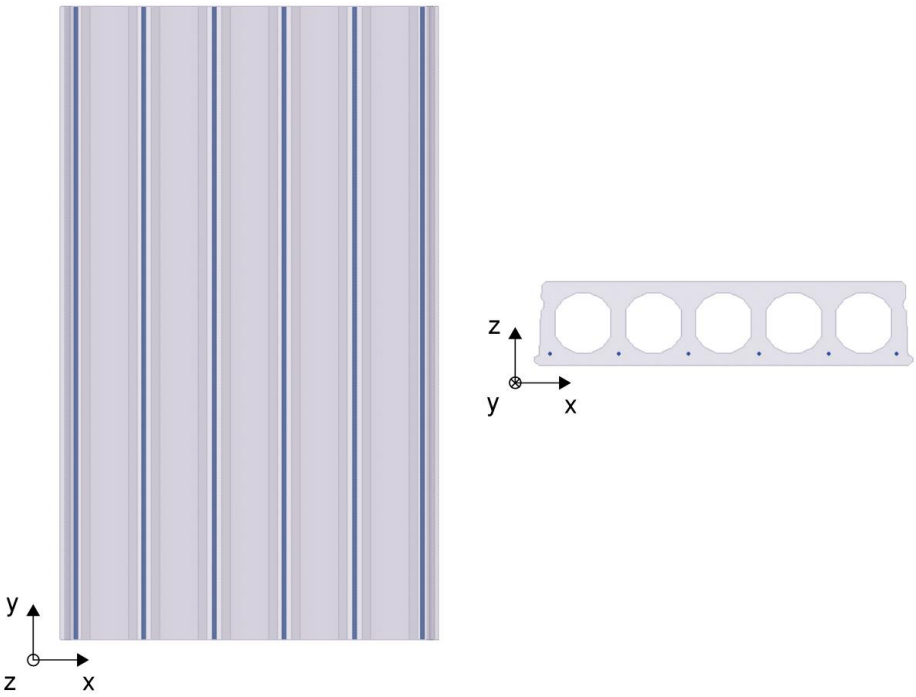

Figure 2.2 A hollow core unit with five voids and six pretensioning steel wires, plane and cross section. 3D directions are defined.

In Figure 2.2, it can also be seen that x-, y- and z-directions have been defined. This is done to simplify the understanding of the differences of how the HC units carries in-plane forces. In the x-direction, the load is transmitted through the HC unit by the flanges and in the y-direction the forces are transferred through the webs.

In a structure, the HC units are commonly supported by placing the short edges on concrete walls. The HC units and the concrete walls are tied together by reinforcement, and then grouted together. How the HC units commonly are supported, can be seen in Figure 2.3.

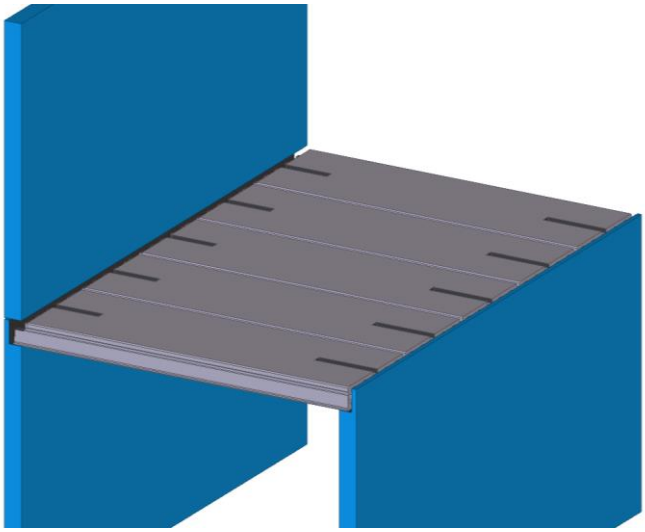

Figure 2.3 The hollow core units are commonly supported by placing the short edges on concrete walls. The walls and the hollow core units are tied together by reinforcement and grout. The recesses for the reinforcement in the hollow core units can also be seen.

2.2 Diaphragm action in floor systems

In cast in-situ structures, the floor systems consist of solid floor constructions. This enables the horizontal forces to be directly transferred to other load-carrying structures without any obstacles. Though, this is not the case for prefabricated concrete floor systems since the joints between the elements can be seen as inconveniences compared to a solid floor system. The ability to create large spans when using prefabricated elements also creates large distances between the bracing units, which in turn impose demands on the design of the prefabricated floor system ((Elliot, 2002) and (Elliott & Jolly, 2013)). A floor system consisting of prefabricated HC units, used to stabilize the structure horizontally, must be designed as a diaphragm and thus act as a plate. This diaphragm sustains forces as shear and bending moments and has the capability of transferring horizontal forces to neighbouring, load-carrying structural members (Fib, 2000). In addition, this means that the floor system constitutes an essential part of the structural system with regard to load transfer (Fib, 2008).

The horizontal forces acting on the facade will give rise to in-plane shear forces in the floor system where the critical parts are the longitudinal joints between the HC units and the joints towards adjacent structural members (Fib, 2014). The in-plane shear forces are transmitted to neighbouring units and other structural members by adhesion and bonding, shear friction, dowel action and mechanical devices which are further described in Chapter 3.2 ((Fib, 2014), (Fib, 2013) and (Elliot, 2002)). As the shear forces have been transmitted through the described joint, they will thereafter end up in connections, e.g. placed at the longitudinal edge of the outermost element towards a load-carrying, neighbouring element, to ensure the diaphragm action. According to Figure 2.4, this is also the location, e.g. towards a shear wall, where a maximum value of shear forces can be found and is thus the most critical section with regard to shear capacity (Fib, 2014).

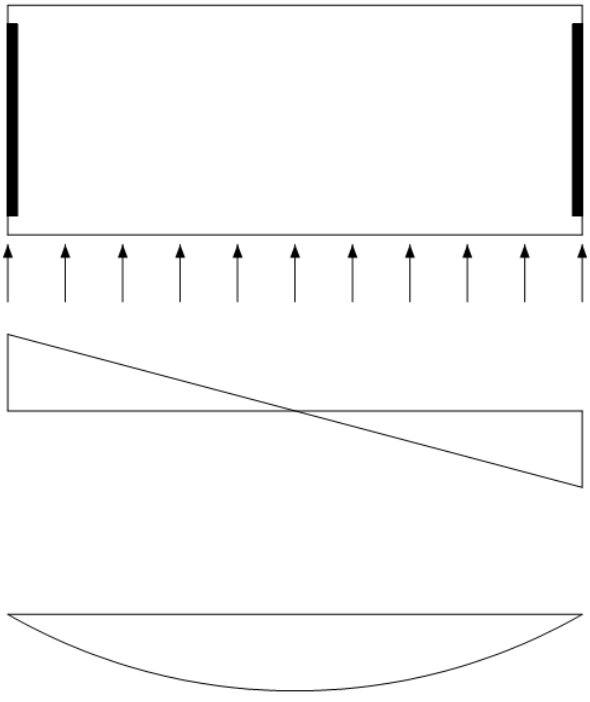

Figure 2.4 Shear and moment diagram of a floor system. Redrawn from Fib (2000).

Depending on how the bracing units, for example shear walls, are placed in a structure, the diagrams of shear and bending moment of the floor diaphragm differs. In Figure 2.5, two additional examples can be seen of how it is affected by the locations of the bracing units. Figure 2.5a shows a case with an internal shear core while Figure 2.5b shows a case with both an internal shear core and a shear wall which are used to brace the structure (Elliot, 2002). Even though examples in Figure 2.4 and Figure 2.5 only show the distribution of forces in the same directions as the load is acting, it is as important to design the floor in the perpendicular direction (Fib, 2000).

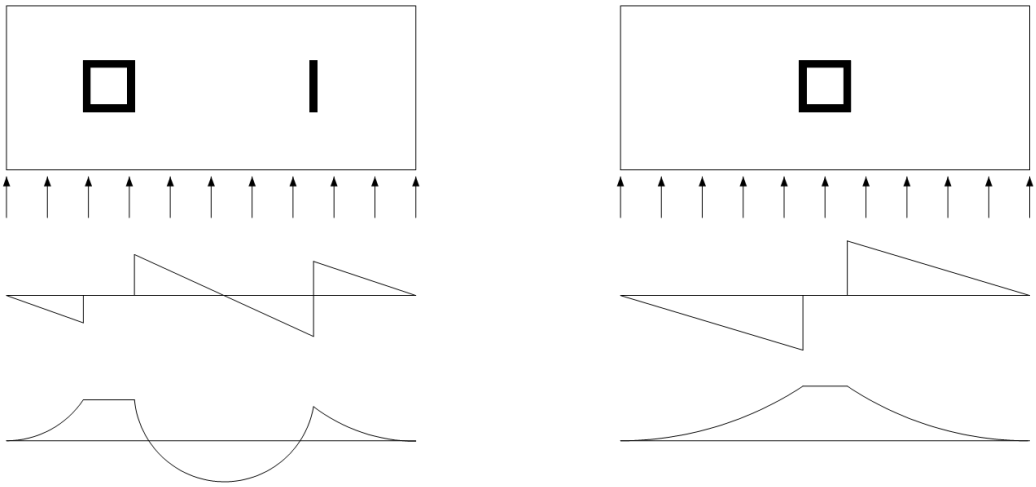

Figure 2.5 Shear and moment diagrams of a floor system with a) an internal shear core and a shear wall, b) an internal shear core. Redrawn from Fib (2000).

The forces acting on the diaphragm is transferred similarly as in a truss, girder or as in a deep beam (Elliott & Jolly, 2013), but is mainly dependent on the geometry of the floor (Elliot, 2002). To describe the transfer of forces, various structural models can be used. Which structural model is most appropriate can be determined by the ratio of the length and width. Depending on this ratio, "Vierendeel girder action" or truss model might be preferred instead of modelling the diaphragm as a horizontal deep beam. Independently of what structural model is chosen, the most critical part of the diaphragm are the joints between the elements or the joints towards adjacent members, which must be able to transfer shear loads to fulfil the desired diaphragm action (Elliott & Jolly, 2013).

If the diaphragm is modelled to handle the load as a truss, the load is transferred diagonally through the HC units and horizontally through the joints between the units, see Figure 2.6a (Fib, 2000). In contrast, the structural model "Vierendeel girder action" takes care of the horizontal loads acting on the diaphragm by a compression and a tensile chord. These chords constitutes of reinforced concrete or beams designed for this purpose (Elliott & Jolly, 2013). This action is illustrated in Figure 2.6b. The third structural model that can be used to describe the shear force transfer in a diaphragm is to perform a model as a horizontal deep beam with tensile and compressive arches. In all these models the shear walls or shear cores acts as supports (Fib, 2000). In Figure 2.6c, a simple case where the diaphragm is modelled as a deep beam is shown.

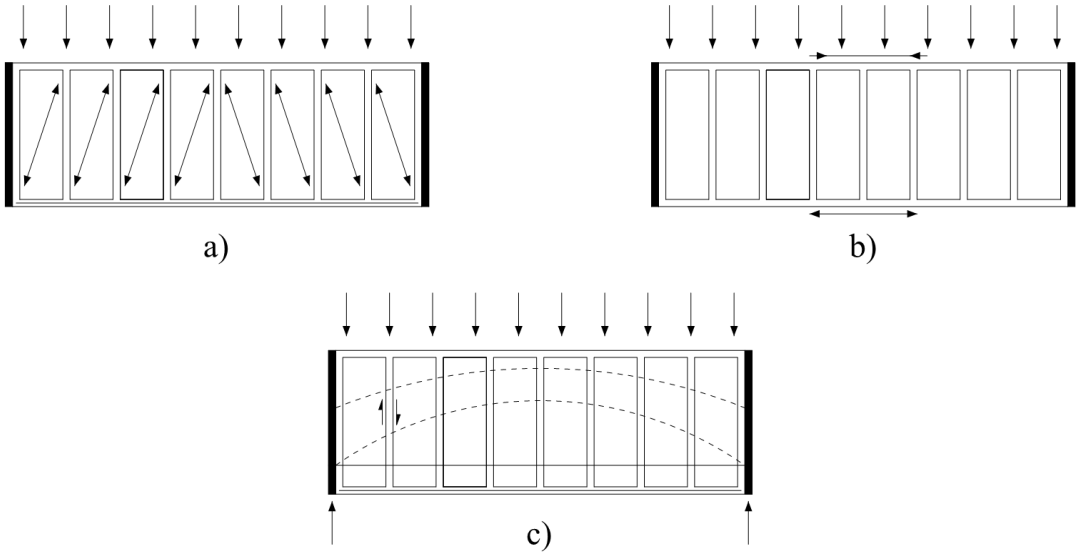

Figure 2.6 Structural models showing the transfer of forces in diaphragms modelled as a) a truss, b) a girder, and c) a deep beam. Redrawn from Fib (2000).

3 Connections

The purpose of connections in prefabricated structures is to provide stability and transfer forces through adjacent structural elements, thus the connections are of great importance in these kinds of structures (Elliot, 2002). A connection is affected by adjacent structural members, which means that the design procedure not only can take the connecting devices into account. The design also needs to regard the joints, including joint faces and joint fill, between the structural elements, together with the end zones of the elements (Fib, 2014). Therefore, a connection is described as an assembly of a number of interfaces and pieces of adjacent elements, which is designed to resist the effect of forces or moments (Fib, 2008). A connection, satisfying all its demands, can be achieved in different ways, e.g. by welding, grouting or bolting. Irrespective of what type of connection, the most important part is that a failure of a connection should not lead to structural instability (Elliot, 2002). The connections need to be designed to resist shear, tension, compression and movements. Some connections also need to be able to withstand a combination of these actions (Fib, 2008).

The desired behaviour of the structural connections is ductility. By a ductile behaviour of the connections, the conditions for cooperation between the surrounding structural elements increase in the stage of fracture, and at the same time the whole structure becomes more resistant to accidental loads and extreme strains (Engström, 1983). The connection's mechanical behaviour is characterized by a relationship between the transmitted force and its following displacement. The maximum allowed displacement for a connection without reaching total degradation, is the deformation capacity. With regard to ductility, the capability of sustaining plastic deformations without decreasing the capacity for resisting forces, is measured for the connection (Fib, 2008).

3.1 Connections in floor diaphragms

In order to fulfil diaphragm action, it is important that the floor units are prevented to move apart from each other (Elliott, 2000). Floor systems composed of HC units should therefore be connected in the joints between the individual elements by tying systems in all in-plane directions, to obtain structural integrity (Elliott & Jolly, 2013). These tie systems help the structure to act as a continuous plate and is thus necessary to achieve the desired diaphragm action. Except for the tying system it is also necessary to provide the system with sufficient grouting in the joints. In addition, there are also other connections that are needed to ensure this action of tying the system together. Typical connections for this purpose, are located at the supporting edges and at the longitudinal edge of the outermost floor unit towards a load bearing member (Fib, 2008). The latter connection was investigated in this study.

3.2 Shear joints and shear transfer

The in-plane shear forces in a floor system designed for diaphragm action, need to be transferred between the diaphragm and the stabilizing units (Elliot, 2002). When designing a diaphragm consisting of individual HC units, the shear transfer in the floor system is an essential part. The shear resistance is achieved by a combination of aggregate and mechanical interlock, and dowel action. Aggregate and mechanical interlock provide shear strength and stiffness and can be divided into adhesive bonding

and shear friction. Steel components as mechanical devices, crossing the cracked interface, provides structural integrity by dowel action (Fib, 2000).

Shear forces are rarely acting alone across a joint; normally they are transferred in combination with compressive forces across surfaces. Shear joints appear between surfaces of remarkably large areas, as between HC units. The shear transfer is complex and designing these types of joints demand caution. This due to the transfer's dependency on texture of small interfaces, and because shear failure is brittle and not elastically recoverable (Elliot, 2002).

3.2.1 Adhesive bonding

If cast in situ concrete is grouted on a precast concrete surface; an adhesive bond develops as the fresh concrete paste penetrates the pores of the mature concrete. This bond is strong in shear alone, but if there are tensile stresses without transverse restraints, a sudden shear failure will take place. Therefore, shear bond is not allowed to act alone (Elliot, 2002). Adhesive bond is not dependent on the smoothness of the surface, but can be reduced by contamination of the surface (Fib, 2013).

3.2.2 Mechanical and aggregate interlock

After adhesive bonding has reached its capacity, a mechanical interlock between the materials cast at different times, prevents the elements from moving apart when subjected to shear (Fib, 2014). In Figure 3.1 mechanical interlock is illustrated.

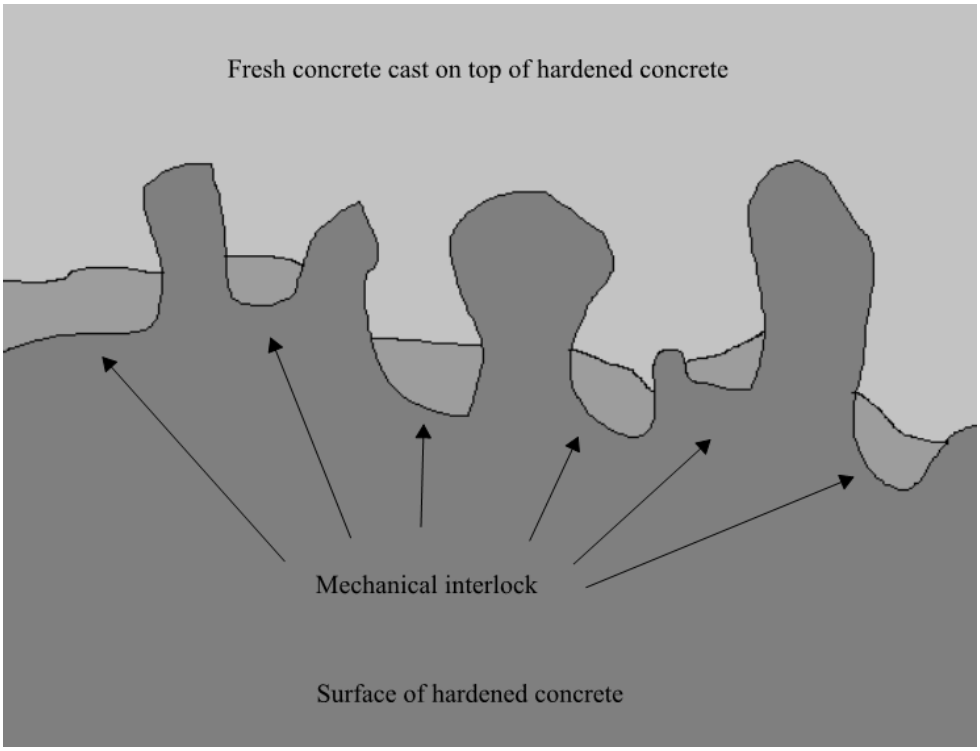

Figure 3.1 An illustration of mechanical interlock when fresh concrete is cast on a hardened concrete surface. Redrawn from de Reese et al. (2013).

In contrast, aggregate interlock takes care of the internal shear transfer within a material. An illustration of aggregate interlock can be seen in Figure 3.2.

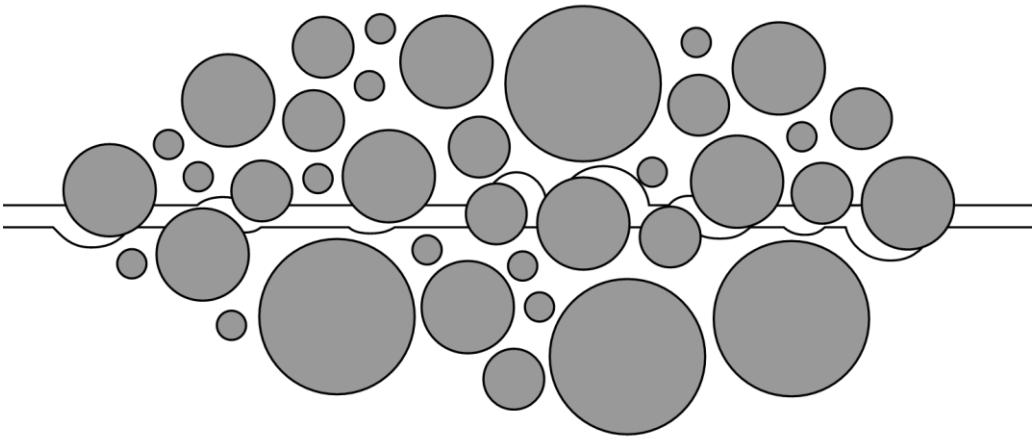

Figure 3.2 An illustration of aggregate interlock. Redrawn from Micallef et al. (2014).

Altogether, the both types of interlock will reduce, or significantly prevent, the shear slip along a joint (Fib, 2014). One type of mechanical interlock is shear friction, which depends on the interface between surfaces in contact. This shear transfer mechanism is dependent on the roughness of a joint which transfers shear by friction - if a compressive force perpendicular to the interface is present (Fib, 2000). The compressive forces can be generated by reinforcement or connectors when they are stretched during shear sliding (Fib, 2013).

3.2.3 Mechanical shear devices and dowel action

Mechanical shear devices, e.g. reinforcement bars, studs or bolts, contributes to local shear transfer. These devices usually consist of steel details, that either are bolted or welded to steel plates or steel beams (Elliot, 2002). The studied connection includes mechanical shear devices and is further explained in Chapter 3.3. When shear forces are transferred through e.g. reinforcement bars, studs or bolts, across a cracked joint, it is called dowel action. This action can be seen in Figure 3.3, and is activated when the interface of the joint is fully cracked, and refers to the bending resistance of the dowel, though the shear slip along the interface generates a lateral displacement which induce bending stresses in the dowel (Fib, 2000). The dowel is embedded in concrete, in which a shear force is acting, and a possible failure mode is local crushing of the concrete in front of the dowel. In turn, due to an increased lever arm, this can lead to a ductile failure in bending. To increase the resistance of dowels, splitting reinforcement is usually placed around them (Elliot, 2002).

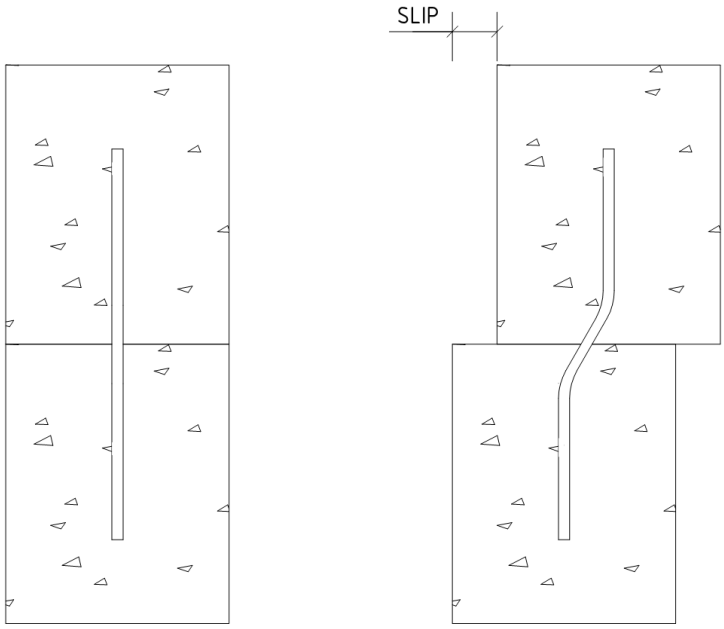

Figure 3.3 A mechanical shear device in steel, crossing an interface of concrete. When the interface is fully cracked and a shear slip takes place, dowel action is activated.

3.2.4 Interaction of shear mechanisms

The various mechanisms of shear transfer often interact and are therefore affected by each other in terms of the shear slip. A shear slip is a difference in lateral displacement of the two surfaces in a joint. Theses mechanisms have maxima at different shear slips. The development of the shear mechanisms starts with adhesive bonding. When the adhesion capacity is reached, shear slip takes place and the adhesion drops significantly and is thereafter not recoverable. As the shear slip increases, the aggregate interlock quickly decreases while the shear friction decreases slightly. When the resistance of the friction decreases further, an increase of the bending resistance of the connecting devices takes place due to larger shear slip (Fib, 2013).

3.3 Studied transverse connection

If the shear force acting along a joint cannot be resisted alone by either adhesive bonding or aggregate interlock, reinforcement or other types of mechanical devices crossing the joint, are required (Fib, 2013).The connection examined in this study includes a mechanical device - a steel component, KBA-5, which comprises of a smooth steel plate of quality S355J2, welded together with two reinforcement bars on top of the plate, see Figure 3.4. The reinforcement bars have the quality K500B and a diameter of 12 mm.

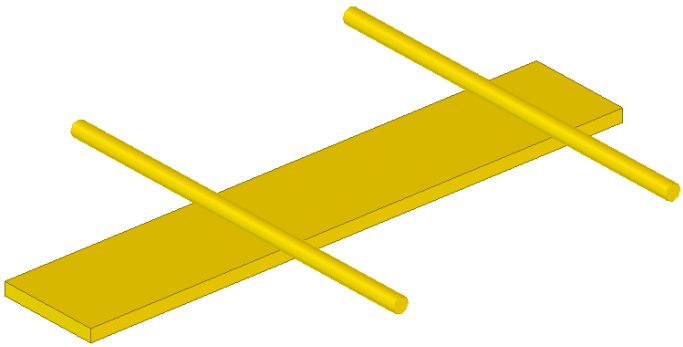

Figure 3.4 The steel component KBA-5, which comprises of a steel plate welded together with two reinforcement bars.

The component is placed inside the HC on site in a recess that is premade at the concrete plant. Each reinforcement bar is placed in one void, the recess is then cast, and the component is therefore of a hidden character in a connection between HC unit and adjacent steel beam. The joint between the HC and the adjacent steel beam is also filled with grout. The location of the studied connection, and the component KBA-5, can be seen in Figure 3.5.

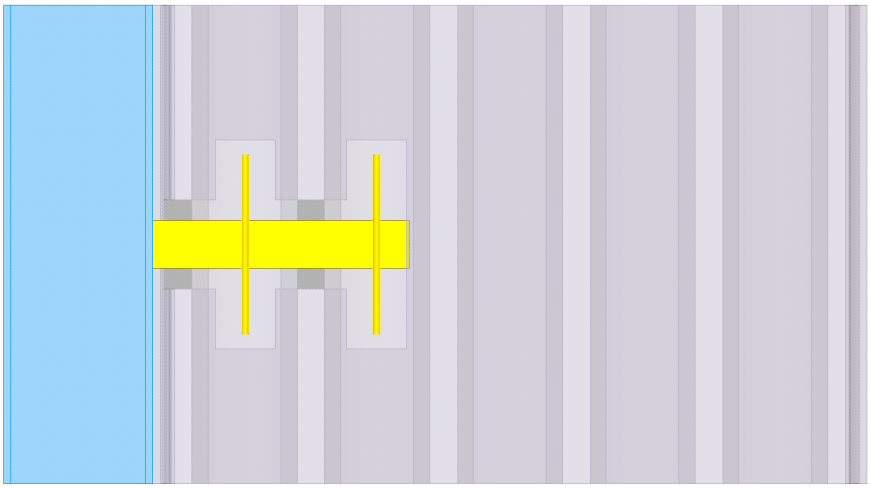

Figure 3.5 The studied connection includes a steel beam, a hollow core element and the steel component KBA-5.

The steel component KBA-5 is, as mentioned, a mechanical shear device and will thus mainly transmit shear forces by local shear transfer (Elliot, 2002). Due to the grout in the joint between the HC unit and the steel beam, adhesive bonds and shear friction will transmit the shear forces. Another possible way to transmit the forces is by dowel action by the steel component.

4 Today's Design Procedure

The common design procedure in the construction industry, regarding the studied connection including the component KBA-5, is presented in this Chapter. The procedure consist of parts of EN-1992-1-1 (2008a), EN-1993-1-1 (2008b), EN-1993-1-8 (2008c) and the Norwegian handbook Betongelementboken (2013), that are considered as important constituents to take into account. In simpler terms, the design of the connection considers the capacity of the HC unit, the grouted concrete and the steel parts, as the component KBA-5 and the related welds. However, today's design procedure does not consider the case investigated in this study. In other words, there is no value of capacity from today's design procedure which could be compared to the results obtained in this study. Thus, this Chapter only presents the procedure of today's design, and no values from the different possible failure modes.

4.1 Design regarding concrete failure

Today's design procedure considers both the concrete of the HC units and the concrete of the grout. In following Sub-chapters 4.1.1 and 4.1.2, parts of this procedure are presented.

4.1.1 Failure mode of the concrete of the hollow core units

Regarding the concrete of the HC unit itself, the possible failure mode is a tensile failure along one void. This design is based on equations and theory gathered from the Norwegian handbook Betongelementboken (2013). In this design, the in-plane tensile capacity of the HC unit is dependent on the tensile strength of a thin, notional concrete plate. In the studied case, the plate is represented by a thickness equal to the thinnest layer of concrete, above or below, the voids. The thickness is illustrated as t_{min} in Figure 4.1.

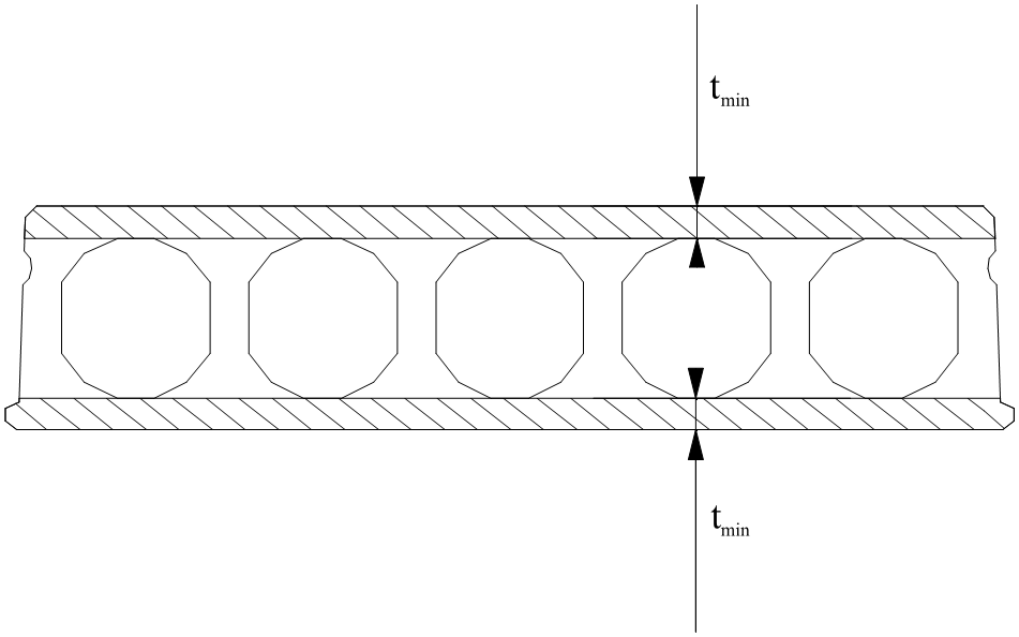

Figure 4.1 The concrete plates of the hollow core unit which the tensile capacity is dependent on. t_{min} represents the smallest concrete thickness, either above or below the voids.

Since it is unlikely that the tensile strength is reached in the concrete both above and below the voids at the same time, only one "plate" represents the capacity. This means that only one layer of concrete can be utilized when a tensile failure occurs and an upper limit of the tensile strength of such a plate is determined by

$$s_{dU} = 0.5 \cdot f_{ctd} \cdot t_{min} \tag{4.1}$$

where

f_{ctd} is the design tensile strength of the concrete.

t_{min} is the thickness equal to the thinnest layer of concrete, above or below the voids.

It should be noted that s_{dU} is an evenly distributed, horizontal force action along one void of the HC unit.

Since the component KBA-5 acts as a point load on the longitudinal edge of the HC unit, the maximum capacity $S_{Rd.c}$, regarding horizontal tensile forces, is determined by multiplying the upper limit value, s_{dU}, with a value of s. This value (s) represents the minimum centre distance between two components, and the length of the notional concrete plate

$$S_{Rd.c} = s_{dU} \cdot s \tag{4.2}$$

$$s = 2 \cdot a + 150mm \tag{4.3}$$

where

a is the penetration length in concrete of the steel component.

The minimum centre distance is illustrated in Figure 4.2.

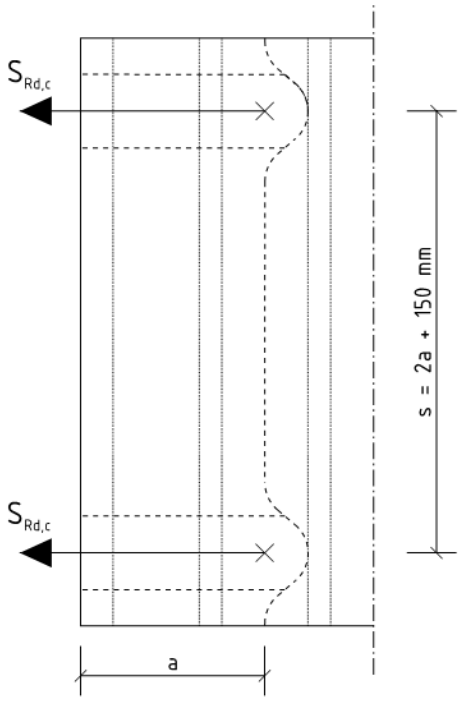

Figure 4.2 The minimum centre distance between two components, s, also represents the length of the concrete plate. $S_{Rd.c}$ is the maximum point load capacity regarding horizontal tensile forces, and a is the penetration length of the steel component. Redrawn from Betongelementforening (2013).

Mathematically, and partly practically too, this means that an increase of the distance a, increases the point load capacity and that the connections can be grouted into the HC units further apart. It is though important to remember that an increase not always results in an increase of the point load capacity, as the failure mode can change. Since HC units individually are considered as one-way spanning concrete elements, they are rather tender for transversal recesses. Because of this, it is appropriate, and recommended, to anchor the component in the second void, as illustrated in Figure 4.2.

Though, the tensile capacity can be used to determine the final, required CC-distance between the connections by

$$s_{Rd} = \frac{S_{Rd.c}}{S_{Ed}} \tag{4.4}$$

where

S_{Ed} is the design tensile force.

4.1.2 Failure modes in the grouted concrete

As mentioned previously, today's design procedure regarding the concrete components, also considers the concrete casted into the recess of the HC unit. The grout is cast at site and a possible failure mode is local crushing of the concrete against the component KBA-5. This design is carried out in accordance with EN-1992-1-1 (2008a).

The design for local crushing considers two different cases, in other words two perpendicular surfaces. The locations of these surfaces are represented by the sectional marks, A-A and B-B, seen in Figure 4.3.

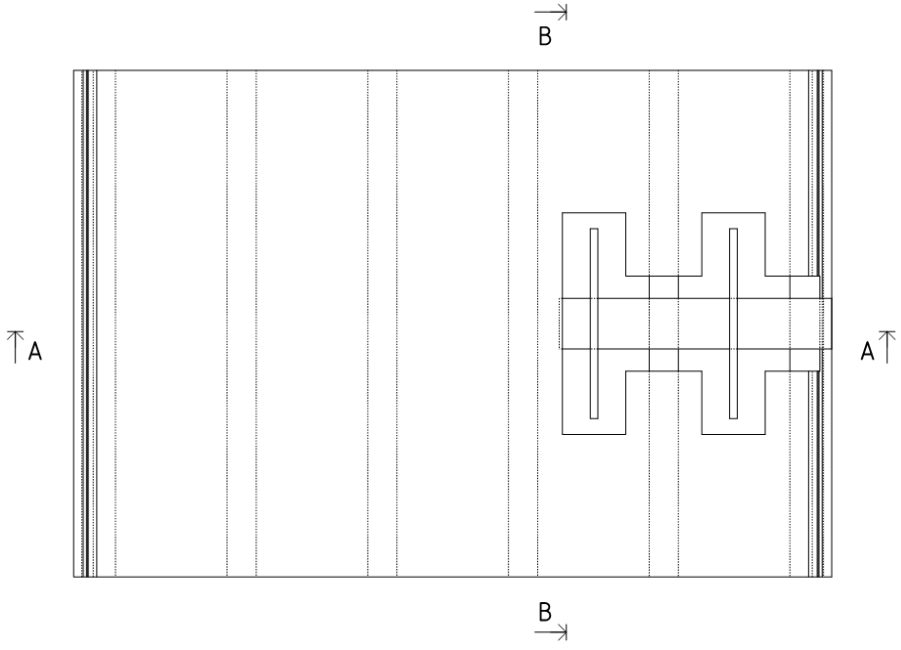

Figure 4.3 Section A and B, showing sections regarding local crushing.

The equation used to determine the capacity of local crushing is according to Equation (6.63) in EN-1992-1-1 (2008a), which is as

$$F_{Rdu} = A_{c0} \cdot f_{cd} \cdot \sqrt{\frac{A_{c1}}{A_{c0}}} \tag{4.5}$$

where

A_{c0} is the loaded area

f_{cd} is the design strength of concrete

A_{c1} is the maximum distribution area with the same shape as A_{c0}.

The different areas used in the equation are illustrated in Figure 4.4. The values of b_2 and d_2 are assumed to be of their maximum allowed value, and thus three times bigger than the dimensions for the loaded area.

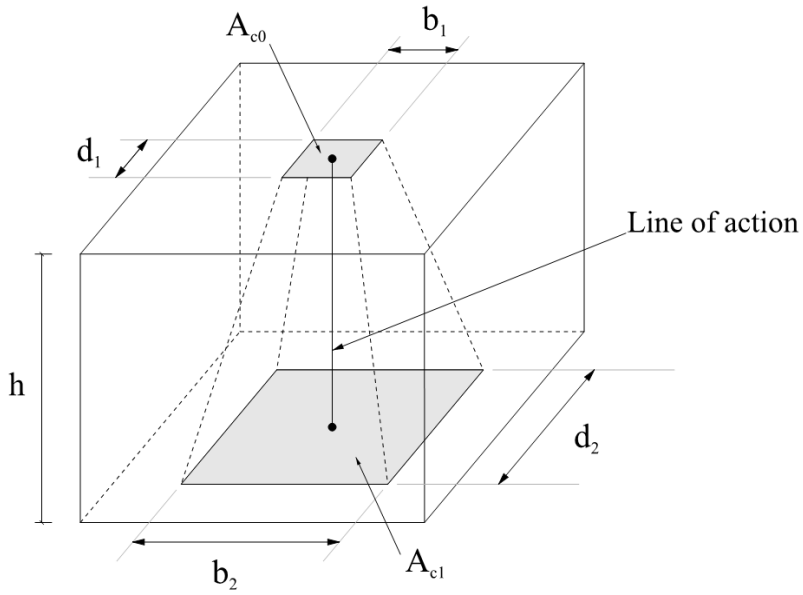

Figure 4.4 Illustration of the areas A_{c0} and A_{c1}, used to determine the capacity of local crushing. Redrawn from Swedish Standards Institute (2008a).

This means that the areas used in the equation are rewritten as

$$A_{c0} = b_1 \cdot d_1 \tag{4.6}$$

$$A_{c1} = b_2 \cdot d_2 = (3 \cdot b_1)(3 \cdot d_1) = 9 \cdot b_1 \cdot d_1 = 9 \cdot A_{c0} \tag{4.7}$$

where

b_1 is the width of the loaded area

d_1 is the length of the loaded area

b_2 is the width of the maximum distribution area

d_2 is the length of the maximum distribution area

In turn, this means that the used Equation (4.5), is simplified and rewritten as

$$F_{Rdu} = 3 \cdot A_{c0} \cdot f_{cd} \tag{4.8}$$

It should though be noted that this also is the maximum allowed capacity according to EN-1992-1-1.

When considering the capacity of section A-A, the loaded area, A_{c0A} , is represented by the length and thickness of the steel plate of KBA-5, marked with red colour in Figure 4.5.

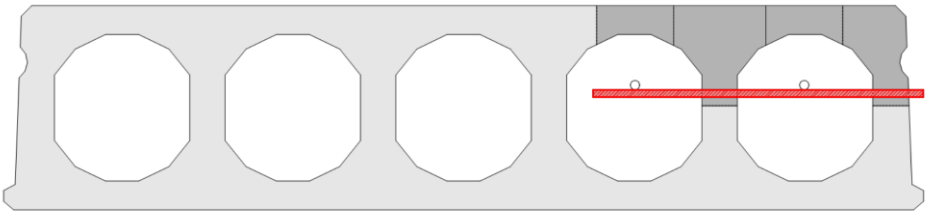

A – A

Figure 4.5 The surface, marked in red, of the steel plate of the component KBA-5, affecting local crushing of concrete.

In section B-B, the loaded area, A_{c0B}, comprises the diameter of one steel bar, multiplied by the width of the steel plate, marked with red colour in Figure 4.6.

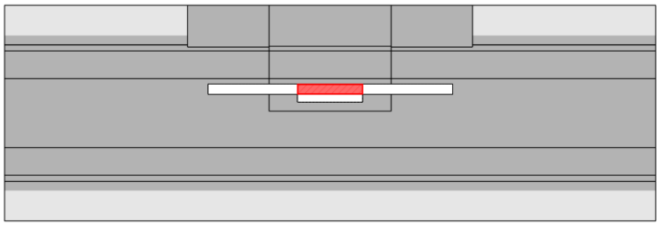

B – B

Figure 4.6 The surface, marked in red, of the steel bar of the steel component KBA-5, affecting local crushing of concrete.

4.2 Design regarding failure in steel component and weld

When performing the design of the steel component KBA-5, three different design procedures are considered to ensure sufficient capacity of the connection. These concern the capacities between the;

- Steel beam and the end of the steel plate of component KBA-5.
- Welds located between the steel beam and the plate of KBA-5.
- Welds between the steel bars and the plate.

In this study, only the capacity of the parts in concrete are considered, which means that the capacities given by the steel parts, including the welds, are neglected. Therefore, the design procedure regarding the steel parts is not presented further.

5 Alternative Design Approaches

The existing design approach for the studied transverse connection, is today based on part of codes and regulations. These parts are assumed to reflect the structural behaviour of the connection, mainly based on engineering assumptions. To extend the understanding of the structural behaviour and to be able to identify opportunities for improvement, alternative design approaches were analysed.

In this Chapter, basics of suitable alternative design approaches for the studied connection are presented.

5.1 Strut and tie method

A useful method to understand the flow of forces within a reinforced or prestressed concrete section, is the strut-and-tie method, which is a lower bound approach (Fib, 2013). This method is based on general principles, various assumptions and rules. Thus, one design problem can have different proposals of strut and tie models. This is due to that only equilibrium conditions and strength limits for the elements need to be fulfilled, but not compatibility (Fib Working Party 1.1.3, 2011).

In the strut and tie model, B- and D-regions are defined, as can be seen in Figure 5.1. In the B-regions (Bernoulli regions), the stresses can be seen as linearly distributed and the Bernoulli hypothesis of a linear strain distribution can be applied through the whole B-region (Engström, 2015). The D-regions are discontinuity regions coming from geometrical discontinuities as frame corners or openings, from concentrated loads as support zones or anchorage of prestressed tendons, or from a combination of both (Fib Working Party 1.1.3, 2011). In the D-regions, the stress and strain distributions are not linear, instead they are dispersing across the section. Therefore, other methods than the Bernoulli hypothesis must be utilized in these regions (Engström, 2015). The structural connections of a precast concrete element have both geometrical and static discontinuities, and these connections zones can thus be defined as D-regions. A strut-and-tie model can therefore be utilized for structural connections and thus generate the needed arrangement of the specific components of the connection (Fib, 2008).

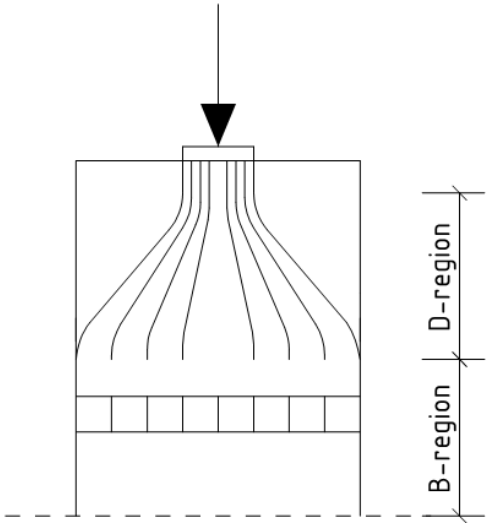

Figure 5.1 B- and D-regions in a concrete member. The stresses are linearly distributed within the B-region, while this is not the case for the D-region. Inspired by Engström (2015).

The intention of the strut and tie model is to estimate the stress field in the ultimate limit state for cracked reinforced concrete, and is thus based on theory of plasticity (Engström, 2015). Despite this, a strut and tie model generally shows a stress field that reminds of linear elastic response. The reasons behind this, are the limited ability for plastic redistribution of reinforced concrete and that the design needs to generate a good performance in the service state too (Fib Working Party 1.1.3, 2011).

The first stage of developing a strut and tie model can have two approaches; the load path method combined with rules for the configuration of the strut and tie model, or by using results from a linear FE analysis (Engström, 2015). The latter approach is though not used in this study.

The load path method shows the resultant of the stress field in every section (Fib, 2013). To avoid a load path that is too simplified for the structure, the stress fields can be divided into several different parts where each part has their own load path. Of course, the load path method must take equilibrium conditions into account. Where a load path changes its direction, transverse forces are acting. If the path is changed in a sharp bend, the transverse force is concentrated in that point and if the bend is softer, the transverse forces are distributed within an area. The load paths also need to follow the same direction as the support reaction or the applied load at the boundary. Another condition with regard to load paths is that they cannot cross each other (Engström, 2015). See Figure 5.2 for the development from a stress field to a load path.

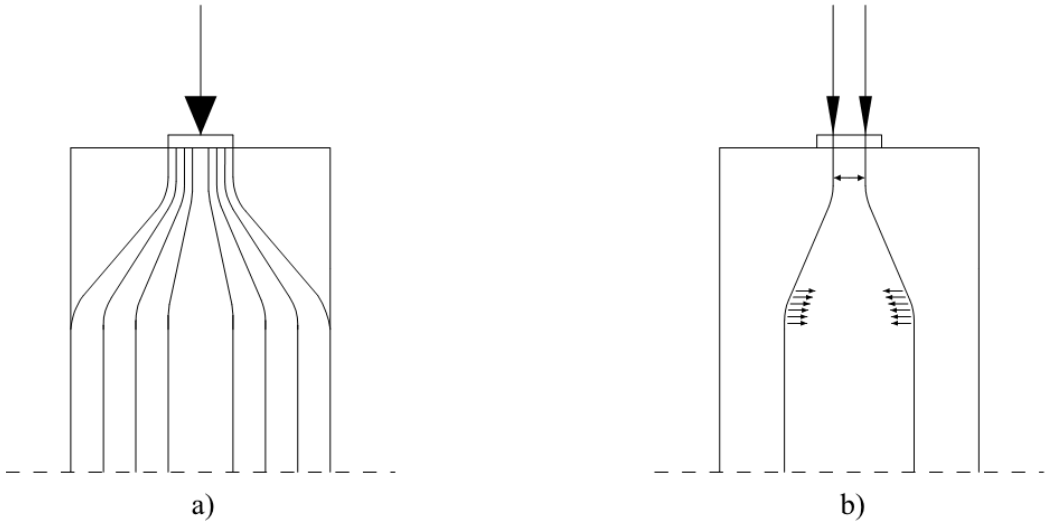

Figure 5.2 The development from a) the stress field in the section, to b) a resultant of the stress field with transverse forces where the load path bends. Inspired by Engström (2015).

When a reasonable load path is specified for the structure, the strut and tie model can be developed, see Figure 5.3. Where the load paths change direction, node points are inserted and between these, struts or ties are located. Ties (full lines) represent tensile forces in the structure and struts (dotted lines) represent compressive forces (Engström, 2015).

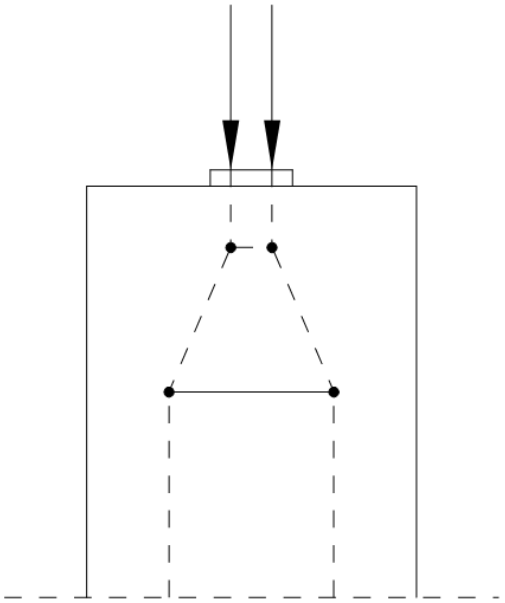

Figure 5.3 The strut and tie model, based on a load path with node points inserted between the struts and ties. Dotted lines represent compression and full lines represent tension. Inspired by Engström (2015).

When a structural member is designed based on the strut and tie model, there are some application rules to follow in order to fulfil a desired behaviour in the service state and with regard to ductility. These rules relate to the deviation angles under concentrated forces and between struts and ties. For example, the angle under concentrated forces should be between 30° - 45° as the stresses should disperse as soon as they have entered the D-regions (Engström, 2015).

5.2 Longitudinal edge joint

Another way of achieving a design value with regard to shear force is to design the connection by Equation (6.25) in EN-1992-1-1 (2008a). This equation ensures that the capacity of the joint, filled with grout at site, is sufficient compared to the applied force. Thus, this design method only considers the capacity of the joint including a part of the steel component, connecting the HC unit to the surrounding load-carrying structure. Equation (6.25) in EN-1992-1-1 is as follows

$$v_{Rdi} = c\, f_{ctd} + \mu\, \sigma_n + \rho\, f_{yd}\,(\mu \sin\alpha + \cos\alpha) \leq 0.5\, \nu\, f_{cd} \quad (5.1)$$

where

c is a roughness parameter

μ is a roughness parameter

σ_n is the minimum external force per area acting perpendicular to the joint

ρ is the ratio between the area of the steel component and the loaded area

f_{yd} is the design strength of steel

α is the angle of how the steel component is crossing the joint

ν is a reduction factor

f_{cd} is the design strength of concrete.

Values of the material parameters, as tensile and compressive strength of the concrete and the yield strength of the included steel component, can be found in tables or by previously made tests of the specific components.

In Equation (5.1), the values of c and μ are dependent on the roughness of the included interfaces. The roughness of different interfaces are classified according to four different categories; very smooth, smooth, rough and intended, in ascending degrees of roughness (Swedish Standards Institute, 2008a); see Table 5.1 for specific values.

Table 5.1 The values of c and μ dependent of the roughness of the interfaces.

Roughness	c	μ
Very smooth	0.025-0.1	0.5
Smooth	0.2	0.6
Rough	0.4	0.7
Intended	0.5	0.9

The value of ρ is calculated as the ratio between the cross-section area of the included steel component crossing the joint, A_s, and the loaded area of the joint, A_i

$$\rho = \frac{A_s}{A_i} \quad (5.2)$$

The angle α is visualized in Figure 5.4 and should be limited by $45° < \alpha < 90°$. Thus, this angle represents the configuration of how the steel component crosses the joint.

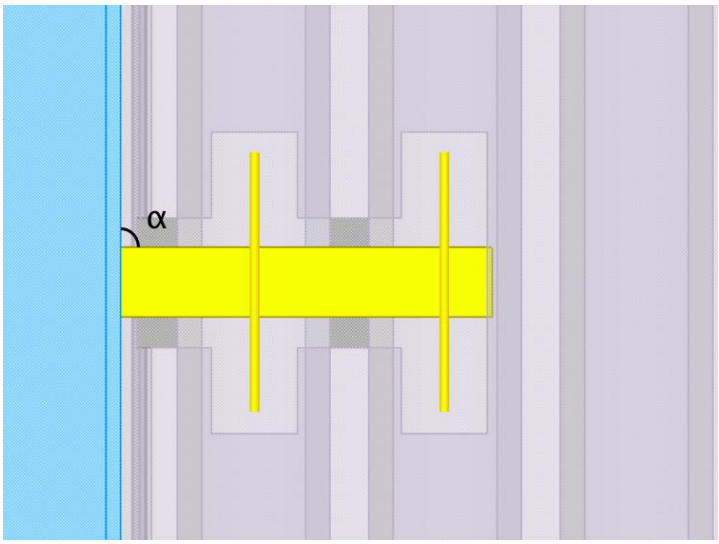

Figure 5.4 Alpha is representing the angle of how the steel component KBA-5, is crossing the joint.

As can be seen in Equation (5.1), the final value of v_{Rdi} should not exceed a certain value. This value comprises of the compressive strength of the concrete which is reduced by multiplying with a factor of 0.5. The third factor, ν, of this value represents another strength reduction factor which is calculated as in Equation (6.6N) in EN-1992-1-1 (2008a) as

$$\nu = 0.6 \left[1 - \frac{f_{ck}}{250}\right] \qquad (f_{ck}\ in\ MPa) \tag{5.3}$$

where

f_{ck} is the characteristic strength of concrete.

5.3 Structural testing methods

To understand the structural behaviour and validate hand calculations and FE-analyses of connections, experiments are appropriate to use (Naito & Ren, 2013). Existing experiments considering connections in prefabricated HC units, are mostly performed where the actions of vertical loads results in transversal shear force failures. These tests are performed at the support edges of the units and at the same location, it is also common to evaluate pull-out failures due to horizontal forces (Engström, 1983). The pull-out test measures the required force to pull out a certain component out of the concrete it has been cast into (Bickley & Engineers, 1986). A model of a pull-out test can be seen in Figure 5.5.

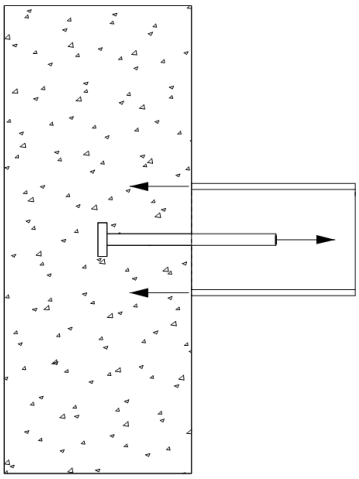

Figure 5.5 An illustration of how a pull-out test is performed. Inspired by Bickley and Engineers (1986).

To experimentally evaluate the connection placed at the longitudinal edge of the HC unit, towards a neighbouring load-bearing element, a push-out test is regularly used. The standard push-out test measures the slip between a steel beam and two concrete slab portions, that are connected to the steel beam through shear connectors, see Figure 5.6. It is either measured by displacement or load increments, and results in a load-slip curve that characterizes the behaviour of shear connectors ((Swedish Standards Institute, 2009) and (Bouchair et al., 2012)).

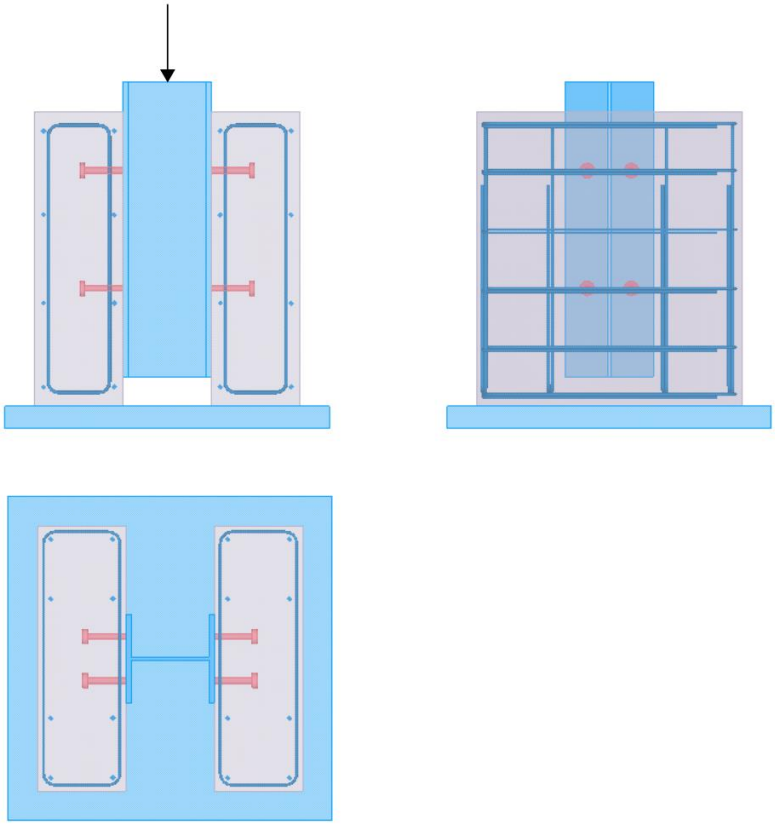

Figure 5.6 A push-out test. Redrawn from Swedish Standards Institute (2009).

Experimental investigations have been carried out to test the shear strength of concrete interfaces cast at different occasions. The experiments performed in a small scale have been carried out as slant shear tests, pull off or push off tests (Fib, 2013). A shear slant test can be seen in Figure 5.7, and is performed by subjecting an interface of two concrete semi-prisms in bond, to compression and shear (Naderi, 2009). Observations during these tests gave knowledge about decisive parameters affecting the load bearing capacity. Some examples of the observed parameters are the roughness of the interface, the strength and quality of the concrete, contaminations of surface, eccentricity of shear force, pre-cracking before testing and the ratio of mechanical devices and reinforcement crossing the interface (Fib, 2008).

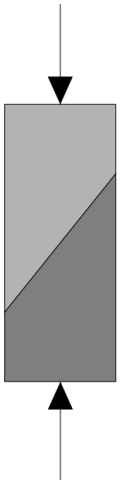

Figure 5.7 A shear slant test of a concrete interface where the two concrete materials, represented by the deviation in shade, have been cast at different occasions. Redrawn from Naderi (2009).

6 Test Setup

A structural test of the connection including the component KBA-5, would not only give a broadened understanding of the structural behaviour, it would possibly also quantify the load bearing capacity. This Chapter presents the limitations, mainly depending on the test machine, that had to be considered when the test arrangement was designed. Furthermore, factors affecting the structural behaviour are analysed, and based on this, a final test arrangement is presented.

6.1 Limitations

The structural test was performed at the factory of KPAB in Uddevalla, Sweden. Due to limitations of the testing machine and costs of performing the test on a real structure, it was not possible to make a full-scale test. The available test machine at KPAB was an Elematic EL465 which is specially assembled for the company. The machine is normally used to check the shear capacity of the produced HC units. In Figure 6.1, an illustration of the machine and how it is regularly used, can be seen.

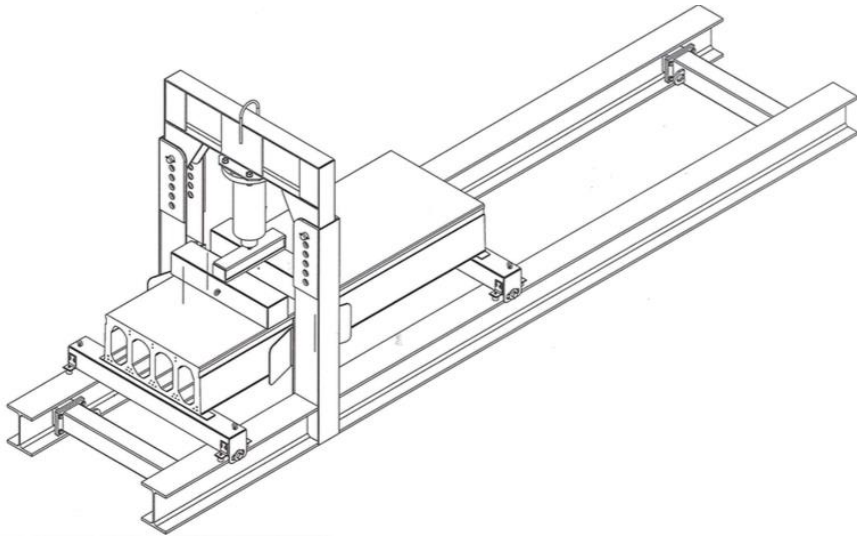

Figure 6.1 The test machine, an Elematic EL465, at Kynningsrud Prefab AB's factory in Uddevalla. The machine is regularly used to check the shear capacity of the produced hollow core units.

The test machine resulted in some limitations when planning how the test was to be performed. One main limitation regarding the machine, was the possibility to only apply a vertical load on the test specimen. In other words, the test specimen had to be placed vertically instead of horizontally, as it is done in reality, to reflect in-plane shear forces. Another limitation regarding the machine, was the free height. The chosen length of the test specimen had to be adapted to not exceed the free height, which in this case was 1050 mm. This in turn led to another limitation; as much of the free height was desired to be used for the HC units, to make them as long as possible, which made it possible to only, directly apply the load in one point of the specimen. Thus, a modified push test method, as mentioned in Chapter 5.3, was used.

6.2 Components of test specimen

As mentioned, the studied connection includes components as a steel beam, a HC unit, the steel component KBA-5 and the grout used in the recess and the joint between the steel beam and the HC unit.

Based on the limitations previously mentioned in Chapter 6.1, the test arrangement was assembled as illustrated in Figure 6.2. The use of symmetry simplifies the system and the understanding of the behaviour and was in this case achieved by attaching two HC units to one steel beam. Thus, the applied load was equally divided between the two HC units.

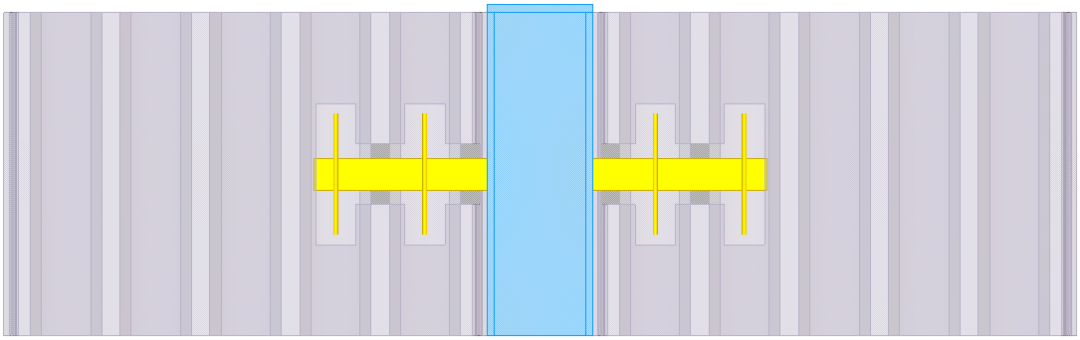

Figure 6.2 The test specimen when two hollow core units are attached to a steel beam through the steel component KBA-5.

Specific details of the dimensions of the components used in this study, are covered by following Sub-chapters 6.2.1 and 6.2.2.

6.2.1 Concrete components

The HC units used in this study were produced at KPAB's concrete plant, with a standard width of 1196 mm. The dimensions of the HC units are shown in Figure 6.3.

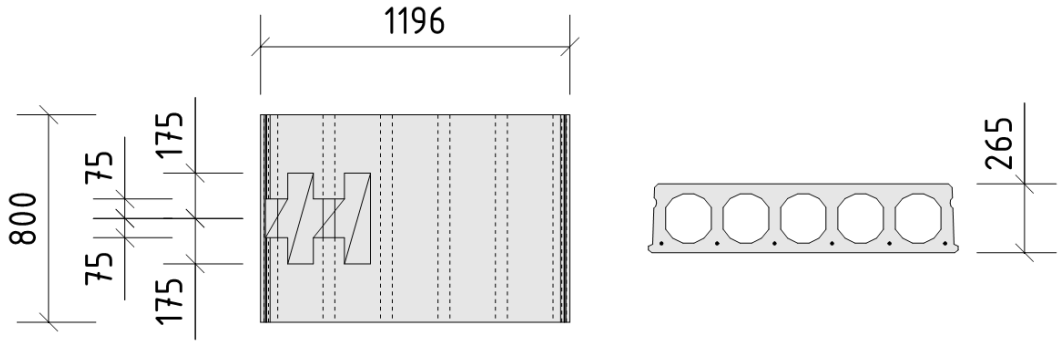

Figure 6.3 Components in concrete of test specimen; HC265. The dimensions of the recess for the component KBA-5 can also be seen to the left.

The concrete mix used can be seen in Table 6.1.

Table 6.1 The mix for the concrete of the hollow core units, used in the test.

Strength	C45/55
Cement - CEMEX Rapid Cement	350 kg/m^3
Water	147 kg/m^3
Additives - VR; GRACE Quantec PL500	2.1 kg/m^3
Aggregate (Crushed concrete 0-16 mm)	35 kg/m^3
Aggregate (Fröland 0-4 mm)	140 kg/m^3
Aggregate (Fröland 8-16 mm)	175 kg/m^3

The concrete strength of the elements was aimed to be C45/55. Cube tests, carried out after 28 days of curing, showed an average strength value of 60.4 MPa. From this, the average compressive strength was determined as (Al-emrani et al., 2013)

$$f_{cm} = \frac{f_{cm.cube}}{1.2} \tag{6.1}$$

where

$f_{cm.cube}$ is the average compression strength from cube tests.

1.2 is a conversion factor to transform the cube value into a cylinder value.

The characteristic strength of the concrete was determined as (Al-emrani et al., 2013)

$$f_{ck} = f_{cm} - \Delta f \tag{6.2}$$

where

$\Delta f = 8\ MPa$

The characteristic strength was used to calculated the mean value of the tensile strength from Table 3.1 in EN-1992-1-1(2008a) as

$$f_{ctm} = 0.3 \cdot {f_{ck}}^{2/3} \tag{6.3}$$

for concrete strength ≤ C50/60

These results are compiled in Table 6.2.

Table 6.2 The average strength from three cube tests, followed by the average compressive strength, the characteristic strength and the mean value of the tensile strength, of the concrete used for the hollow core units.

$f_{cm.cube}$ [MPa]	60.4
f_{cm} [MPa]	50.3
f_{ck} [MPa]	42.3
f_{ctm} [MPa]	3.6

The units included six pretensioned steel wires with a diameter of 12.9 mm which were tensioned to a force equal to 90 kN and placed 35 mm from the bottom of the HC. The depth of the HC units was 265 mm and the length 800 mm, which was, as mentioned, chosen to fit the free height of the machine. The recess, in which the component KBA-5 was placed, was grouted at a later occasion than the HC units, and the concrete used for the grouting of the recess was aimed to have the strength FB450. The mix used for the grout can be seen in Table 6.3.

Table 6.3 The mix for the grout, used in the test.

Strength	FB450
Cement – Rapid Cem 1 52.5	450 kg/m^3
Water	202.5 kg/m^3
Additives – Sika Viscocrete	3.4 kg/m^3
Aggregate (0-4 mm)	1675 kg/m^3

After 28 days of curing, cube tests of the grout were carried out; these showed an average strength value of 44.6 MPa. The average compression strength, the characteristic strength and the mean value of the tensile strength, were determined by Equation (6.1), (6.2) and (6.3). These values are compiled in Table 6.4.

Table 6.4 The average strength from three cube tests, followed by the average compressive strength, the characteristic strength and the mean value of the tensile strength, of the concrete used for the grouting.

$f_{cm.cube}$ [MPa]	44.6
f_{cm} [MPa]	37.2
f_{ck} [MPa]	29.2
f_{ctm} [MPa]	2.8

6.2.2 Steel components

The steel beam was a HEA260, chosen in correlation with the dimension of the depth of the HC units, in steel quality S355. On top of the steel beam, a steel plate with dimensions of 245x245x20 mm, in the same quality as the steel beam, was placed. This was done to spread the force evenly into the steel beam, since it was the member which was subjected to direct loading. The steel component KBA-5 is described in Chapter 3.3, and was welded to the steel beam at the same location as the web of the beam. This to minimize negative effects, which could be brought about if welded at the flange of the beam. The connections of the steel components can be seen in Figure 6.4.

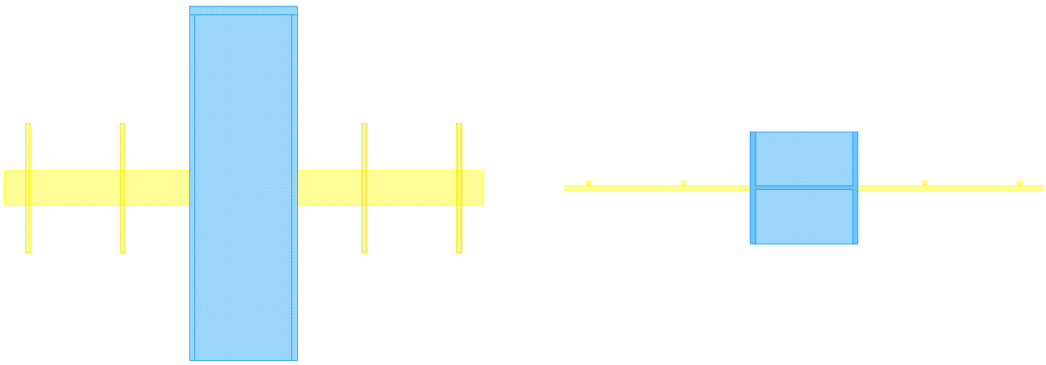

Figure 6.4 Steel components of the test specimen; steel plate, HEA260 and KBA-5. The component KBA-5 was welded to the HEA260, while the steel plate was placed on top of the HEA260.

6.3 Configuration of boundary conditions

Different configurations of the boundary conditions (BC's) in the test setup, affects the results differently; therefore, it was of high importance to evaluate how these would influence the behaviour of the connection in the test. The influence of the BC's are factors that are dependent on choices made based on following Sub-chapters 6.3.1 and 6.3.2, in contrast to the limitations explained in Chapter 6.1, that had to be followed.

The factors influencing the results in this case were identified as the support conditions, the placement of the supports, and finally, whether to use a plastic sheet between the steel beam and the HC unit, or not.

6.3.1 Conditions and placement of supports

Two possible support conditions were identified for this test arrangement. One possible support condition was to have the HC ends placed on steel plates, on top of steel cylinders which in turn, would be resting on steel plates. To ensure safety for the persons involved when performing the test, the steel plates under the cylinders would have edges to counteract too large movements. Another option, easier to perform, was to place the edges of the HC units, directly on steel plates only. Both options can be seen in Figure 6.5.

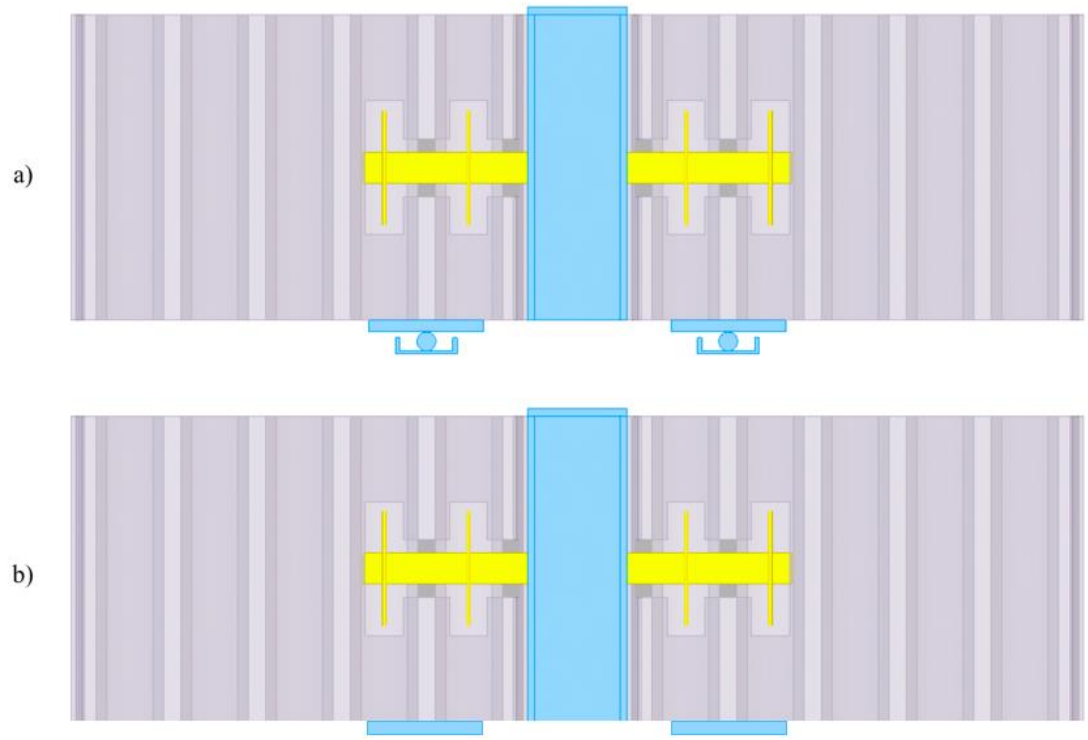

Figure 6.5 Different support conditions where the hollow core units in a) are placed on steel plates, on top of steel cylinders, resting on steel plates with edges, and in b) resting on steel plates only.

If the HC units would be placed on steel plates only, friction would occur between the concrete and the plates. The placement of the steel plates, regardless location at the edge of the HC, would eventuate in an arching effect. This effect would be larger if the plates were placed at the edge away from the steel beam, and almost none if placed near the steel beam, due the internal lever arm. The effect counteracts a possible deflection of the whole test specimen. In Figure 6.6 this effect can be seen.

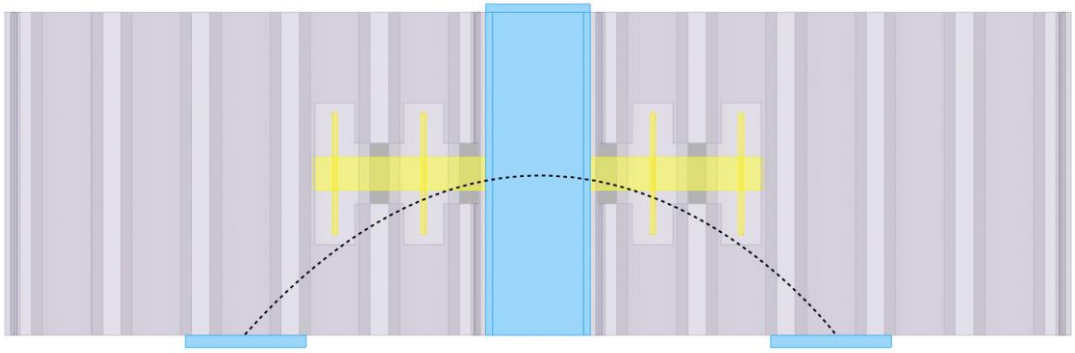

Figure 6.6 If steel plates, alone, are chosen as supports, they generate an arching effect which counteracts a deflection.

If the HC units instead would be placed on steel cylinders on steel plates, no forces due to friction appear; the test specimen is freely supported. The deflections would be larger if the supports were placed at the edge away from the steel beam, due to a larger moment. If the supports were placed near the steel beam, the self-weight of the specimen would initially create a moment which would result in that the upper parts of

the HC units would like to rotate outwards. This would though not be a problem, since this moment would be counteracted when the load on top of the steel beam is applied. This position of the supports would also minimize the deflections of the specimen, and result in a more pure shear force acting on the connection, than placing the supports further out from the steel beam.

6.3.2 Plastic sheet between steel and concrete member

The grout in the joint between the steel beam and the HC unit contributes to the shear capacity of the connection and helps the structure to carry applied loads. The contribution of this action is not large, but can be calculated by hand, see Chapter 5.2. However, for the actual behaviour of the shear transfer, there are some uncertainties that need to be handled. If the grout is not performed correctly in reality, it does not provide the structure with the calculated and expected stiffness. In turn, this gives a calculation on the unsafe side. This test could be performed as it is done at site, grouting the longitudinal joint in an ordinary way and perform the comparing calculations by using the factors representing the adhesion action. Another way of performing the test could be to grout the test specimen as it is done at site, but to use plastic sheets between the steel beam and the grouted concrete. This would prevent the adhesion action, and in hand calculations the factors representing this action could be minimized. By doing this, the solutions of the hand calculations and the test would be on the safe side and any contribution from the adhesion action only would increase the stiffness of the structure.

The plastic sheet placed between the steel beam and the HC units prevents, in theory, all friction to occur between the two materials. In practice, this is not the case since friction is a mechanism that is hard to totally prevent.

6.4 Choice of testing arrangement

The factors mentioned in Chapter 6.3, were chosen to reflect a real behaviour of a connection exposed to laterally in-plane shear forces, and to make the BC's easy to identify in a future FE-analysis.

The most appropriate support conditions were found to be the steel cylinders on steel plates. If only steel plates would be used, the force due to friction had to be considered. However, this is a difficult parameter to determine. In other words, using steel plates alone, was not preferred. Another reason in favour of using steel cylinders as supports, were easy identification of the BC's.

In a real structure, the forces in HC units are distributed over the whole width of the elements. By the chosen support condition, this is not the case in this test since the HC units rest on steel cylinders, which generates a concentrated stress field at this location. To see how these stress concentrations would influence the connection, two different support locations were chosen. In one, the supports were placed at the second web in relation to the steel beam, see Figure 6.7a. The other support location was to place the supports at the fourth web, see Figure 6.7b. This was done to force the loads to transfer differently into the component KBA-5. In the first case, the load can be directly transferred from KBA-5 through the second web, to the support. In the second case, the load must be transferred from KBA-5 into the flanges of the HC unit, before it reaches the fourth web and thus the support.

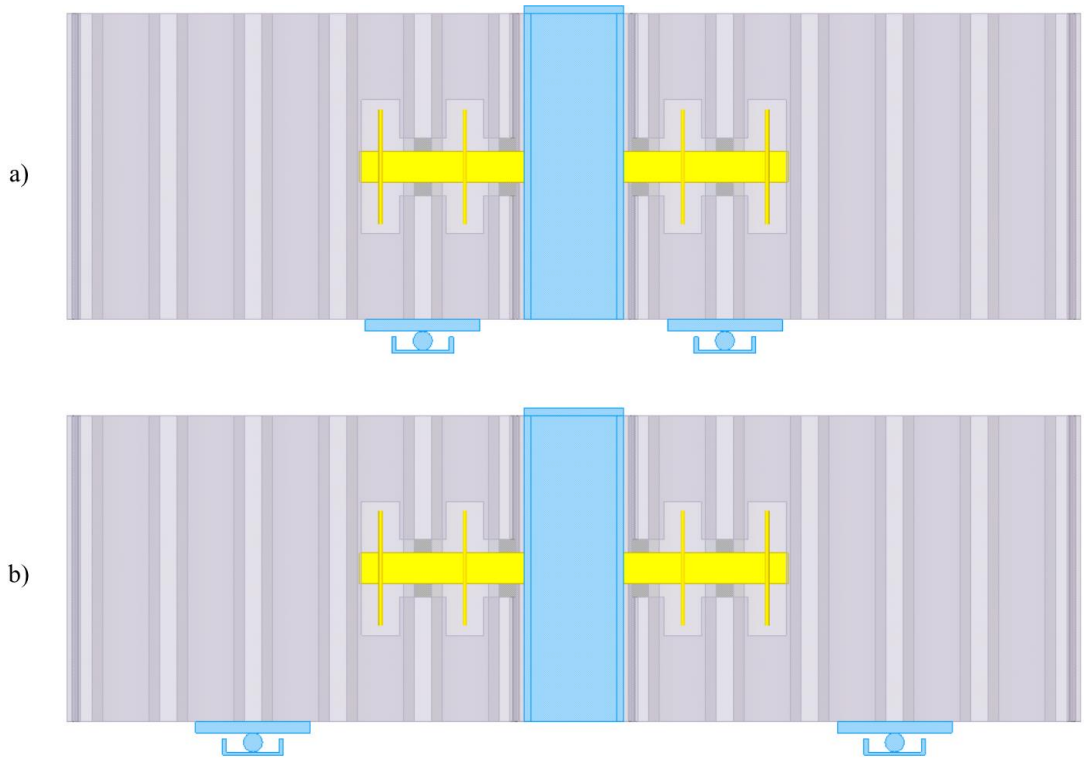

Figure 6.7 The supports were placed at two different locations when performing the tests. The locations were a) at the second web, and b) at the fourth web, in relation to the steel beam. The aim was to see how the concentrated stress field affected the connection.

When the supports were located at the second web, the load transfer was presumed to only depend on half of the width of the HC units; the half adjacent to the steel beam. Therefore, a decision of performing the test on both half width HC units, see Figure 6.8, and on full width, was made. By doing tests on both sizes, it should be possible to see if the load transfer worked as predicted.

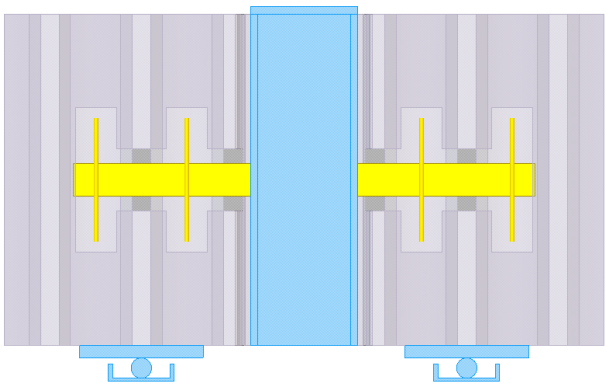

Figure 6.8 Half width hollow core units were also used in the structural tests, though the load transfer was predicted to only depend on these parts.

Independently of the support locations, there was a small influence of rotation, from the moment that appears due to the horizontal eccentricity between the position of the supports and the applied load. By this, the upper part of the HC unit was subjected to horizontal compressive forces regarding the rotational movement, which in turn can result in a possible compressive failure of the concrete. Another possible consequence due to the rotation, is deformation of the component KBA-5.

To simplify the calculations and obtain results on the safe side, a plastic sheet between the concrete and the steel member was used. The plastic sheet prevents, in theory, shear friction to occur, which means that the shear force capacity would not be overestimated.

7 Performance of Structural Tests

To gain knowledge about the structural behaviour and to quantify the load-bearing capacity of the connection including the component KBA-5, a structural test was performed. This Chapter presents the designed test arrangement and how the test was performed.

7.1 Test arrangement

The arrangement of the test was based on Chapter 6, where both the initial conditions and factors affecting the test in different ways were considered. The result from this, was a test specimen composed of a steel beam, HEA260, that was welded together with the steel component KBA-5. On top of the steel beam, a steel plate was placed. The HC units had a length of 800 mm and a width of both 1196 mm and half the width, 598 mm. The joint between the HC units and the steel beam, as well as the recesses for the steel component KBA-5, were filled with grout. The supports had two locations; at the second web of the HC and at the fourth web. The tests with support location at the second web were performed with both halves of the HC units and full widths. The final test arrangements can be seen in Figure 7.1.

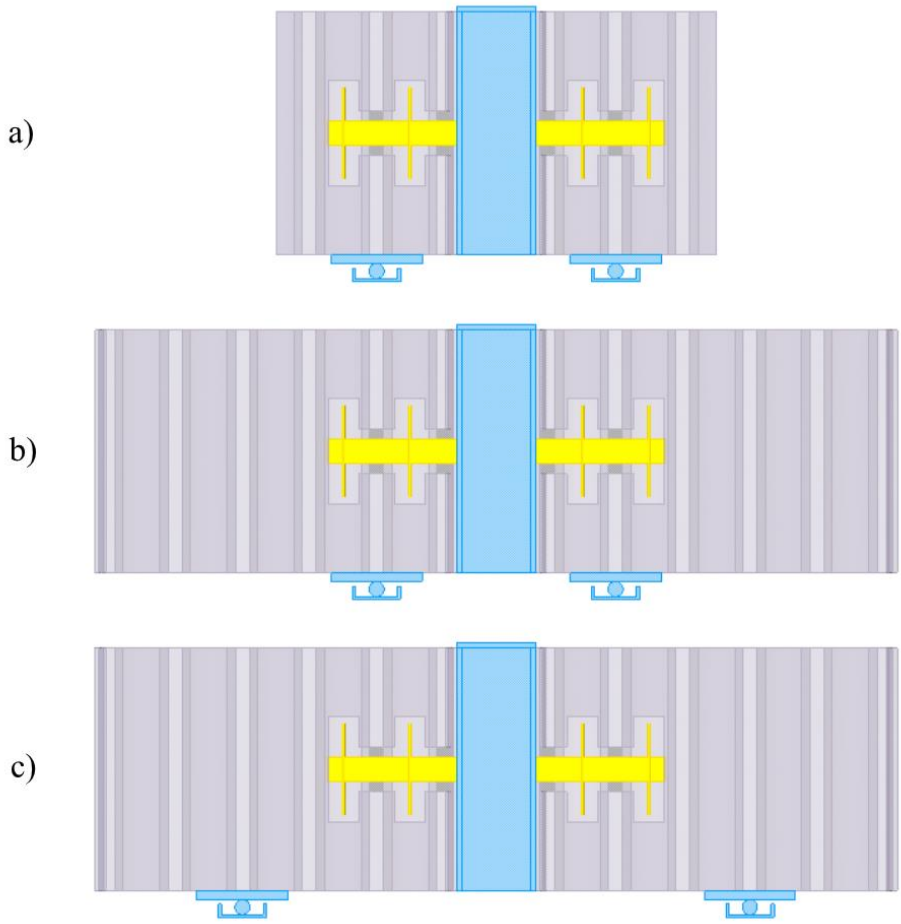

Figure 7.1 The different test setups where; a) half width hollow core units with the supports under the second web, b) hollow core units in full width with supports at the second web, and c) hollow core units in full width with supports at the fourth web.

7.2 Test Performance

The structural test was performed with an Elematic EL465. To place each test specimen in the test machine, a traverse was used. On the two longitudinal steel beams, two transverse steel beams were placed at different distances from the loading point dependent on which support location should be tested. The supports and the test specimen were then placed on the transverse steel beams. To ensure safety, planks of timber were put under the edges of the test specimens to avoid the HC units to fall down when failure was reached. Figure 7.2 to Figure 7.4 show how the test specimens were mounted in the test machine.

Figure 7.2 One test specimen mounted in the test machine, view from the side.

Figure 7.3 One test specimen mounted in the test machine, inclined view from the side.

Figure 7.4 One test specimen mounted in the test machine, front view.

To mainly ensure safety, since the test setup never had been used before, the test session started with a pilot test on a test specimen of half width HC units. The intention was to perform the test with load-controlled loading, with load increments of 10 kN, and to measure the displacement at the different load steps. However, the pilot test showed that it was not possible to perform the loading with increments at all, instead it was only possible to increase the load, by hand, until failure. Therefore, the intended measurement of the displacement was too uncertain since the exact load for a specific displacement could not be achieved, and due to the different speed of the load application. The solution for this problem was to only measure the experimental failure load for each test specimen.

The test specimens were manufactured in a total number of 8 tests. One test specimen was destroyed in the factory due to error in workmanship. The 7 remaining specimens were divided into three half width HC units, and four full width - two with each support location.

Each test was filmed; each HC unit was filmed from one side, see Figure 7.5.

Figure 7.5 Each hollow core unit of the test specimens was filmed by one camera from one side.

The filming from only one side was due to limitations of both number of cameras and space in the factory. Each HC unit was, in the beginning of the test session, marked with a number and a letter to simplify the documentation of the videos. When failure was reached in each test, the test specimen was photographed and documented. It was only the HC unit that reached failure that was documented in photographs. To see how the steel component KBA-5 was deformed in the test, and if it had an influence on how the concrete behaved, the steel component was after some tests taken out from the HC unit.

8 Results and Analysis of Structural Tests

The structural tests were carried out to improve the understanding of the structural behaviour of the studied connection, and to estimate the experimental failure load. This was done by performing structural tests on seven different test specimens which had different properties regarding the dimension of width and support location. The results presented in this Chapter are based on the final crack pattern that can be seen on photos taken at the factory and films from each test session.

To simplify the understanding when reading the results, this Chapter first presents the experimental failure loads, and is further divided into additional Sub-chapters 8.2, 8.3, 8.4 and 8.5, depending on the width of the HC units and support location. In each of the following Sub-chapters, a discussion of the results also can be found.

When referring to the second and fourth web regarding the support location, in the following Sub-chapters, it is in relation to the number of webs away from the steel beam the support was located, see Figure 7.1.

8.1 Experimental failure loads

An overview of all tests can be seen in Table 8.1. It should be noted that the first test was only seen as a pilot test and the result from this is only presented in Table 8.1. In each test, it was only one of the two HC units that reached failure; it is its experimental failure load which is presented in the Table. As can be seen in Table 8.1, the structural response of each test differed mostly regarding the location of the supports and it can also be seen that the average experimental failure load was significantly lower where the supports were located at the fourth web.

Table 8.1 Results from the structural tests, showing the placement of supports, what type of hollow core units were tested, the maximum applied load and the experimental failure load, which is half of the maximum applied load, for each test. Finally, an average experimental failure load for each support location is presented.

	Placement of support	**Type**	**Maximum applied load [kN]**	**Experimental failure load [kN]**	**Average experimental failure load [kN]**
Test 1*	Second web	Half width	369	184.5	-
Test 2	Second web	Half width	445	222.5	200
Test 3	Second web	Half width	311	155.5	
Test 4	Second web	Full width	437	218.5	
Test 5	Second web	Full width	410	205	
Test 6	Fourth web	Full width	200	100	95
Test 7	Fourth web	Full width	180	90	

* Pilot test.

The results of the experimental failure loads, seen in Table 8.1, seems reasonable for two main reasons. The first covers the increase of bending moment when the eccentricity from the applied load increased. The second is due to a longer, and more complex, force path the applied load must be transferred, when the supports were located at the fourth web. The case, where the supports were located directly beneath the second web, is less complex for the force transfer between the steel component KBA-5 and the supports. This since the force can be directly transferred from the steel component, through the grout, into the web and further to the support.

The complexity can be explained by the difference in force transfer in the different directions of the HC units. As mentioned in Chapter 2.1, the forces in the horizontal direction can only be transferred in the flanges, while forces in the vertical direction have their main paths through the webs. This means that when the supports were located at the fourth web, the forces needed to be transferred from the steel component KBA-5 to the flanges, further to the web and finally to the supports.

8.2 Half width hollow core units – support location at second web

In this Sub-chapter, the results from test 2 and 3 are presented. Both test specimens consisted of half width HC units, with supports at the second web.

The results from the photos of the HC units in tests 2 and 3, show similarities in crack pattern on the recess-side. This can be seen in Figure 8.1 and Figure 8.2.

Figure 8.1 The side with recess, of Test 2 after performed structural test. The steel beam where the load was applied, is to the right.

Figure 8.2 The side with recess, of Test 3 after performed structural test. The steel beam where the load was applied, is to the right.

However, the crack patterns on the other side of the test specimens did not appear in the same way in both tests, see Figure 8.3 and Figure 8.4.

Figure 8.3 The side without recess, of Test 2 after performed structural test. The steel beam where the load was applied, is to the left.

Figure 8.4 The side without recess, of Test 3 after performed structural test. The steel beam where the load was applied, is to the left.

When the films from the two test sessions were studied, the difference in behaviour of crack pattern on the different sides, could be analysed. However, the films of test 2 and 3 gave indications on combined bending and shear failures. In test 2 it could, on the film, be seen that the vertical crack propagating in the second void, on the side without recess, started at the bottom side of the HC unit, outside the steel plate, as can be seen in Figure 8.3. Regarding the film from test 3, it could be seen that the HC units slightly were rotating inwards, towards the steel beam, before a complete failure occurred. This rotation, bending, was found causing the inclined failure on the side of the HC unit without recess.

From test 2, the steel component KBA-5 was taken out from the HC unit that reached failure. The deformations of the component showed that it had been subjected to bending and thus a rotation upwards. Since the deformations persisted after the component was taken out of the concrete, it could be presumed that the steel parts had reached yielding and that the mechanical shear device, in terms of the steel component, would contribute to a ductile failure, due to dowel action. The deformation of the steel component KBA-5 from test 2, can be seen in Figure 8.5.

Figure 8.5 The deformations of the steel component KBA-5 in Test 2, after performed structural test. The hollow core unit to the left failed.

If the steel component KBA-5 contributed to any crack formations is hard to ascertain, as there were no data measured of the steel behaviour during the tests. It can be presumed, that the steel component possibly affected the cross-sectional cracks, which is further described in Sub-chapter 8.5.

8.3 Full width hollow core units – support location at second web

In this Sub-chapter, the results from test 4 and 5 are presented. Both test specimens consisted of full width HC units, with supports at the second web.

The photos of the side of the HC units with recesses, see Figure 8.6 and Figure 8.7, show a similar crack in both test specimens. This crack was located vertically at the end

of the recess through the full length of the HC unit, and ended in the centre of the second void of the HC unit.

Figure 8.6 The side with recess, of Test 4 after performed structural test. The steel beam where the load was applied, is to the left.

Figure 8.7 The side with recess, of Test 5 after performed structural test. The steel beam where the load was applied, is to the left.

As well as for the side of the HC units with recesses, the photos of the opposite side also show similarities in crack pattern, see Figure 8.8 and Figure 8.9. When these figures are studied, two main cracks can be seen.

Figure 8.8 The side without recess, of Test 4 after performed structural test. The steel beam where the load was applied, is to the right.

Figure 8.9 The side without recess, of Test 5 after performed structural test. The steel beam where the load was applied, is to the right.

From the films of test 4, it could be seen that the first crack appeared in the first void. In other words, the crack closest to the steel beam, which can be seen in Figure 8.10.

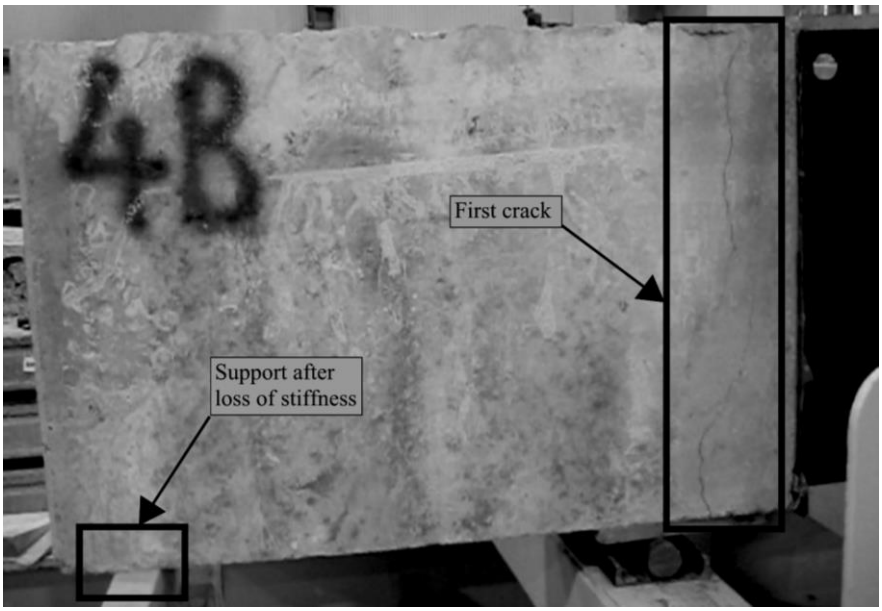

Figure 8.10 The first crack appearing during the test is in the first void. This resulted in a loss of stiffness and that the hollow core unit fell down on the timber planks.

The consequence of the first crack, was loss of stiffness in the concrete of the test specimen, which resulted in that the outer end of the HC unit fell down on the timber planks, that were set up to ensure safety. In other words, the outer end of the HC unit was then resting on the timber planks, which then could be seen as supports. When the applied load further increased, the second crack seamed to appear due to a bending moment caused by the timber planks the outer end of the HC unit was resting on. This can be seen in Figure 8.11.

Figure 8.11 The second crack during the test seemed to appear due to a bending moment caused by that the hollow core unit fell down on the timber planks.

From the film of test 5, it could be noted that the vertical crack started from the top of the HC unit, in contrast to test 4 where it started from the bottom. For test 5, the timber planks, which were used to ensure safety during the tests, were therefore presumed to not significantly affect the test, as the outer part of the HC units were allowed to rotate

outwards, away from the steel beam. The difference in crack propagation of test 4 and 5, can also be seen in Figure 8.8 and Figure 8.9, where the maximum crack opening of the vertical cracks was located at two different locations, in bottom and top, respectively. Although, the vertical crack in test 5 was formed due to loss of stiffness close to the steel beam, as in test 4.

Similarly, as in test 2, the steel component KBA-5 was taken out from the HC unit, which reached failure, in test 4. The deformations of the component showed similarities with the deformations of the steel component from test 2; KBA-5 rotated upwards due to bending and the deformations persisted after being taken out of the concrete. The deformations of the steel component KBA-5 from test 4 can be seen in Figure 8.12.

Figure 8.12 The deformations of the steel component KBA-5 in Test 4, after performed structural test. The hollow core unit to the left failed.

8.4 Full width hollow core units - support location at fourth web

In this Sub-chapter, the results from test 6 and 7 are presented. Both test specimens consisted of full width HC units, with supports at the fourth web.

In test 6, the experimental failure load was reached after a sudden rupture of the HC unit. The crack causing the sudden failure, occurred close to the third web, in other words at the end of the recess, see Figure 8.13 and Figure 8.14.

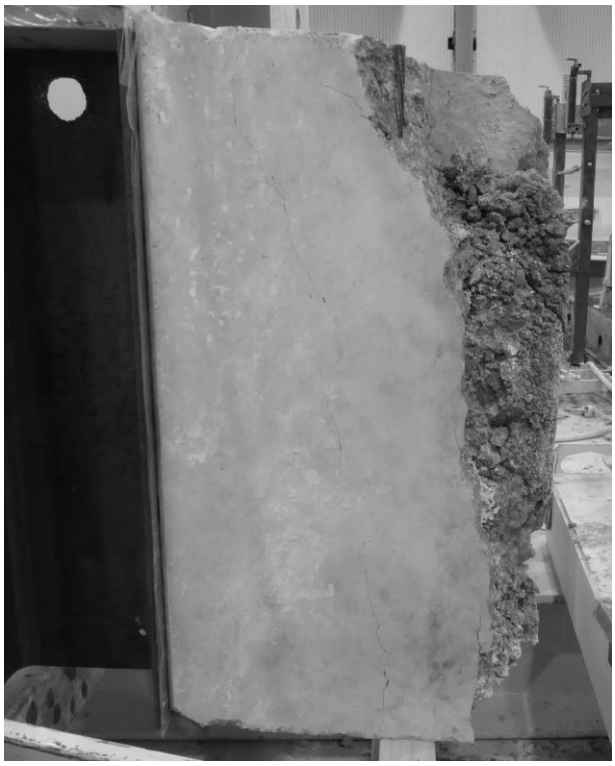

Figure 8.13 The side without recess, of Test 6 after performed structural test. Due to an abrupt failure, only the remaining concrete part, attached to the steel beam, can be seen. The steel beam where the load was applied, is to the left.

Figure 8.14 The side without recess, of Test 6 after performed structural test. Due to an abrupt failure, only the remaining concrete part, attached to the steel beam, can be seen. The steel beam where the load was applied, is to the right.

From the film of test 6 the abrupt failure made it hard to understand what type of failure mode that took place. It could be seen that the HC units were rotating inwards, likely due to the eccentricity between the loading point and the support locations. When the film was studied closely, it could be seen that the crack initiated from the bottom of the test specimen in the centre of the void, which designated on a bending failure. The centre of the void is also where the flange is at its thinnest, and the crack propagation at this location was thus found as a reasonable result. If the complexity of the load transfer, described in Chapter 2.1, is considered together with the crack initiation, the load transfer in the horizontal direction at the lowest part of the second void, could be seen as the failing link and what caused the failure of the test. As the crack propagated upwards in the HC unit, it eventually reached the recess and the grout. At this point, the crack followed the joint between the grout and the HC unit at the outer edge of the recess, which is reasonable since it is the weakest part of this section. Thus, as can be assumed, the mechanical interlock between the grout and the HC unit had a lower capacity compared to the aggregate interlock acting internally in the grout.

From the photos taken of test 7, a crack dispersing from the vertical centre of the HC unit to the centre of the second void, can be noted. This can be seen on both sides of the HC units, see Figure 8.15 and Figure 8.16.

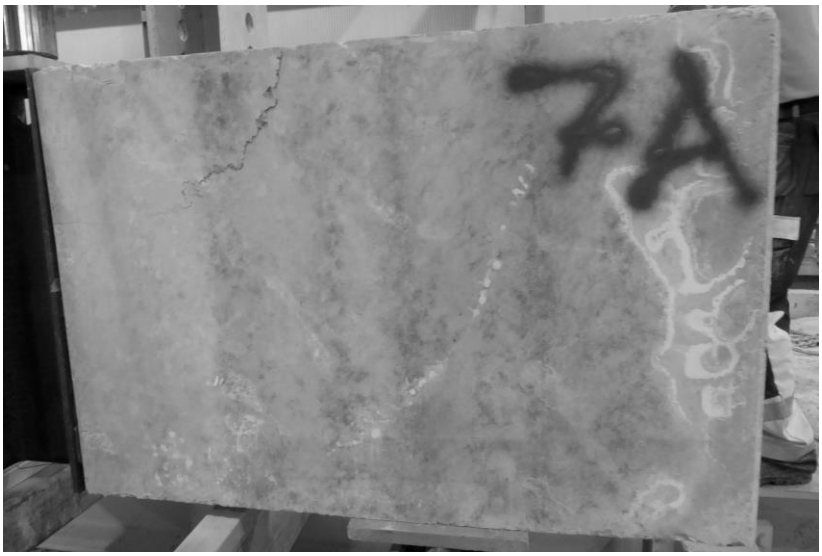

Figure 8.15 The side without recess, of Test 7 after performed structural test. The steel beam where the load was applied, is to the left.

Figure 8.16 The side with recess, of Test 7 after performed structural test. The steel beam where the load was applied, is to the right.

The photos and film of test 7 show a compressive failure, seen in Figure 8.17, caused by bending of the test specimen.

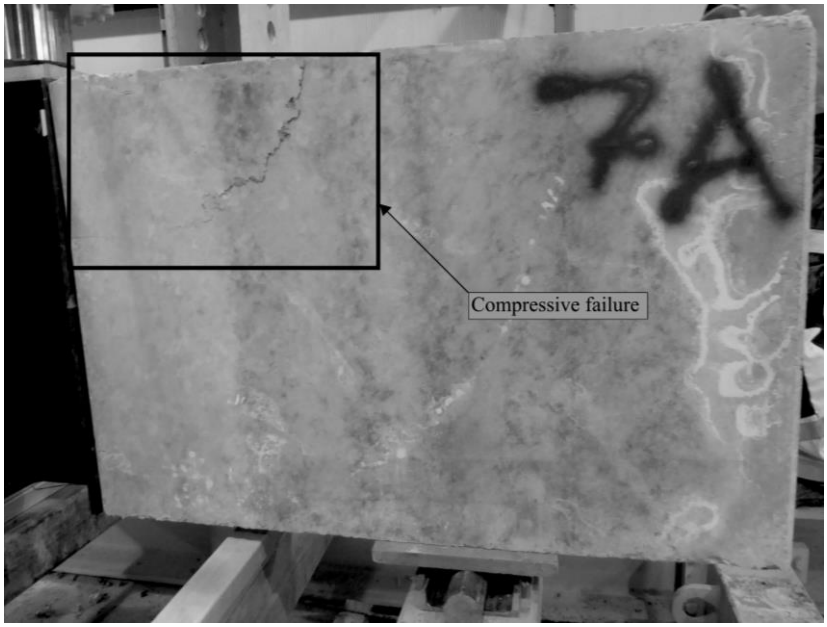

Figure 8.17 A compressive failure in the upper part of the hollow core unit, due to rotation of the test specimen around the steel beam.

8.5 Cross-section of hollow core units

Common for the results for the cross-sectional photos of all tests, were crack formations perpendicular to the two webs closest to the steel beam. The crack widths were of different magnitude, however, the cross-sectional photo showing the most distinct cracks, can be seen in Figure 8.18, which is from test 4. Cross-sectional photos for all tests can be found in Appendix B.

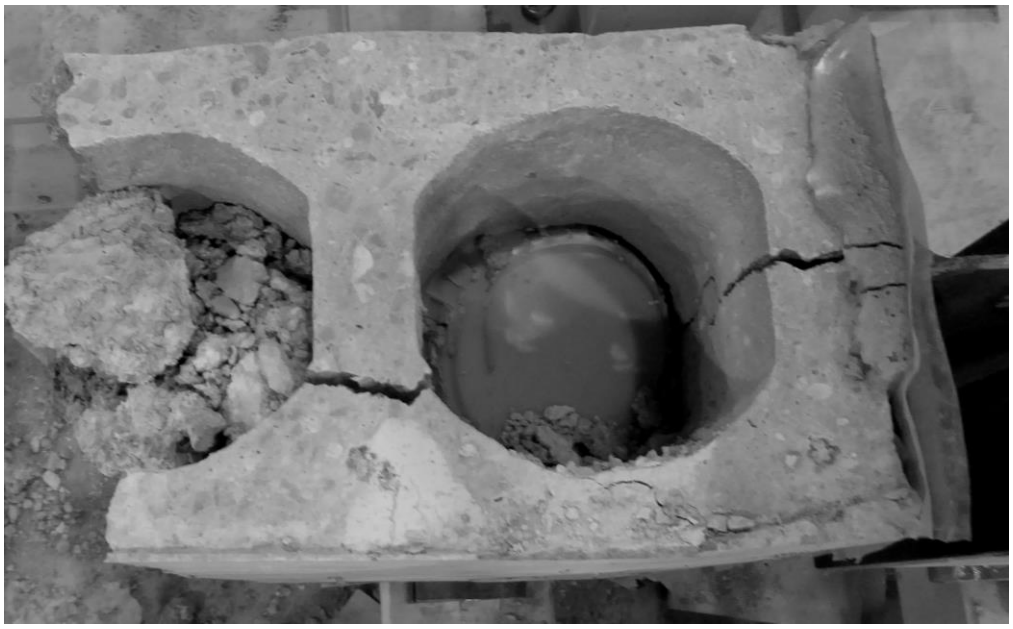

Figure 8.18 The cross-section of Test 4. This represents the general behaviour of the crack formations in all structural tests. The steel beam where the load was applied, is to the right.

The crack in the first web occurred in the centre, while it can be noted that the crack in the second web appeared closer to the bottom flange of the HC unit. This was an overall result that could be noted from the photos of the cross-sections. The motive behind this, was found to be the steel component KBA-5 and the recess. The crack in the first web was located where the steel component was crossing the joint, which could be a result of high concentrated forces from the steel component. Since the area of the steel component crossing the webs, was small in relation to the concrete, the forces did not have the possibility to be distributed to the larger area of the concrete. This possibly generated a knife-like behaviour of the steel component in relation to the surrounding concrete of the HC unit; cracking of the web was a consequence of this. The crack in the second web appeared close to the lower flange, which possibly was due to the recess. Possibly, the crack initiated in the joint between the concrete of the HC unit and the grout, since this is a weak region, due to mechanical interlock. Further on, the crack propagated through the cross-section and reached the top of the HC unit.

9 Analytical Models

As mentioned in Chapter 5, some alternative design approaches compared to today's design procedure, for the studied connection, exist. The results from the analytical design approaches, as the strut and tie method and the calculations of the longitudinal end joint, are presented in the following Sub-chapters 9.1 and 9.2.

9.1 Strut and tie

As mentioned in Chapter 5.1, a strut and tie model can advantageously be utilized to understand the flow of forces within a discontinuity region, as a connection zone. Therefore, a strut and tie model for the test arrangement was conducted to hopefully increase the understanding of the structural behaviour of the studied connection. This would also improve the possibilities of analysing the results from the structural test. In this Chapter, the development of this model is presented.

If a strut and tie model of the connection without the steel component KBA-5 would be developed, it would only be a model in 2D. The presence of the component KBA-5 makes it a problem in 3D, since the force needs to be transferred from the steel beam to the supports through this component, and thus change direction in three dimensions. This results in a rather complex model, which was divided into several steps to reach a final solution.

It should be noted that the Figures in following Sub-chapters, only demonstrates strut and tie models for one side of the test specimen, and were developed together with Björn Engström, Professor at Chalmers University of Technology.

9.1.1 Solid slab in 2D

When performing a strut and tie model for a complex structure, it is advantageous to start with a highly simplified case. For a structure including HC units, it was appropriate to start with simplifications of the concrete elements and see those as solid concrete slabs. Considering the load path of a simplified model, it was suitable to assume that the total force acting on the steel beam, was entering the concrete element only through the component KBA-5. Thereafter, the force was transmitted through the component similarly as in a truss with compression and tensile chords. The load transfer further to the supports, is a typical case of how loads are transmitted to a single point, in a basic strut and tie model as described in Chapter 5.1. This simplified case, subjected the connection zone between the component and the steel beam, to large forces as high moment and shear forces. This, in turn, exposed the concrete in this zone to large tensile and compressive forces. In this case, it was also assumed that there were no shear forces acting in the joint between the steel beam and the concrete slab, which possibly could reflect the behaviour due to the plastic sheet. The simplified and first case, as just described, is illustrated in Figure 9.1.

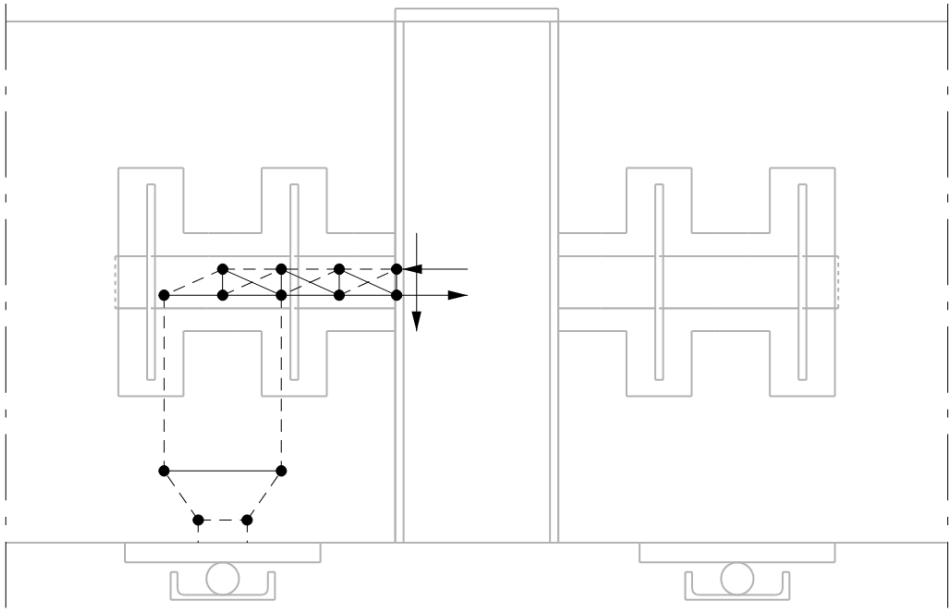

Figure 9.1 . A strut and tie model of a simplified case, where the hollow core units were seen as solid slabs. The steel plate of the component KBA-5 was subjected to shear and bending; no shear forces in the joint between the concrete slab and the steel beam.

Another way of modelling the studied case was to add two compressive struts and one tie above the component KBA-5. This reduced the force couple at the connection zone of the component and the steel beam, due to the compressive resultant in top of the steel beam. In contrast to the first case, the concrete above the steel component was contributing to the resistance of bending moment. Similarly, as in the first case, no shear force in the joint was assumed, consequently all shear forces were transmitted into the steel plate of the component from the steel beam. This second case is demonstrated in Figure 9.2.

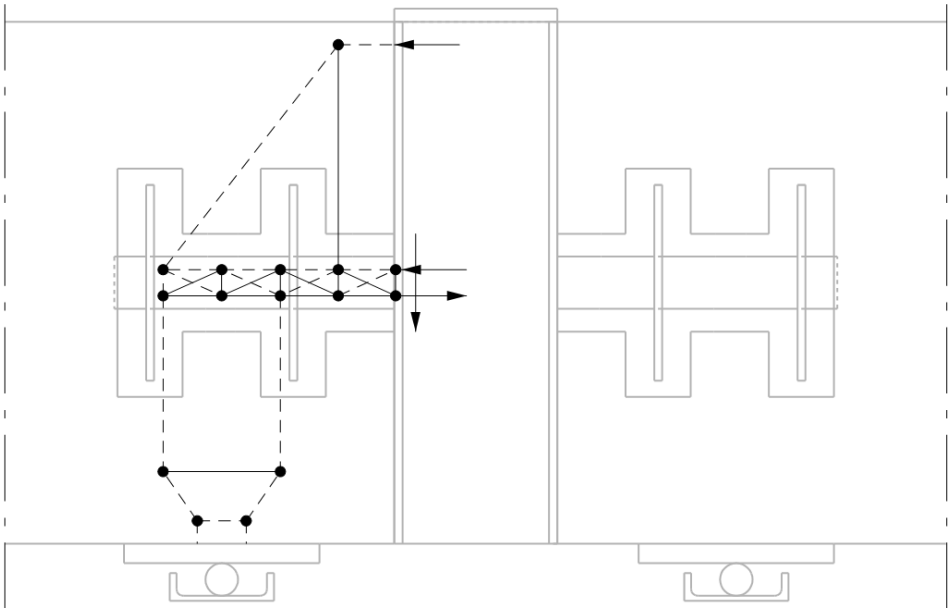

Figure 9.2 A strut and tie model of a simplified case, where the hollow core units were seen as solid slabs. Shear was only transferred through the component KBA-5, while the concrete above the steel component KBA-5 and the steel plate of the component KBA-5, were carrying bending moment.

A third model is similar to the first one, but in this case, it was assumed that the joint between the steel beam and the concrete slab, was fully capable of resisting shear forces. In other words, the effect from the plastic sheet was neglected. This means that the shear resultant directly affecting the component KBA-5, was decreased. Accordingly, this also created a first node placed inside the steel beam, which also was the first location where a load deviation appeared. Similarly, as the second case, the compressive struts above the component decreased the bending moment at the connection zone, at the component and the steel beam, and thus decreased the loads affecting the concrete slab in this zone. Overall, this case exposed the concrete slab to less concentrated loads as forces were acting both above the component KBA-5 and along the joint towards the steel beam. See Figure 9.3 for an illustration of this case.

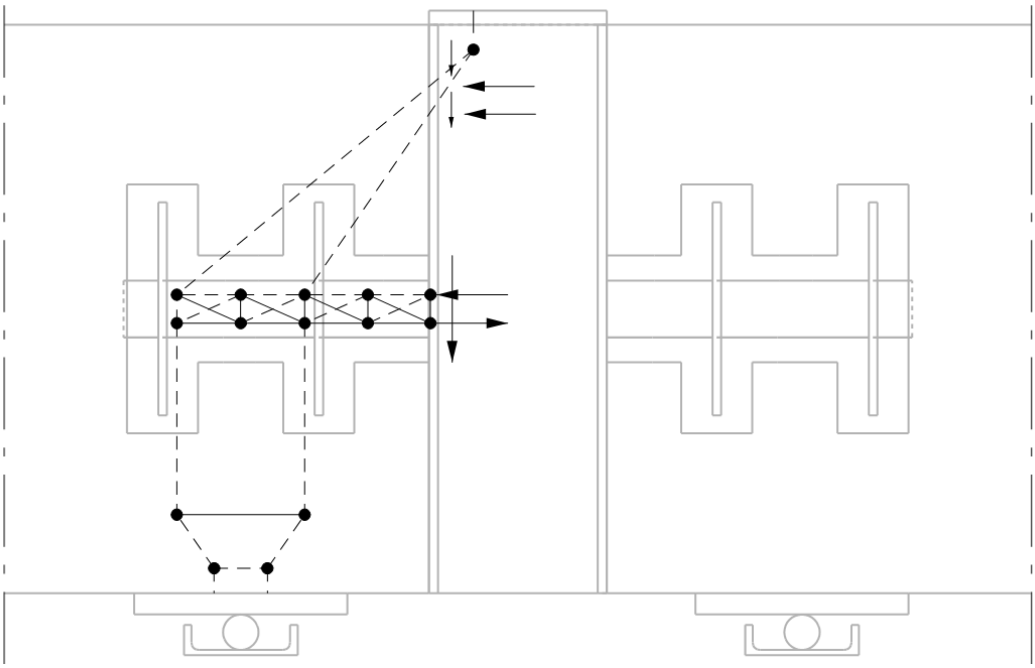

Figure 9.3 A strut and tie model of a simplified case, where the hollow core units were seen as solid slabs. The joint between the steel beam and the concrete slab was in this case capable of resisting shear forces.

9.1.2 Solid slab in 3D

To keep the model of the complex structure simple, the concrete parts of the model were still considered to be solid concrete slabs as in Chapter 9.1.1. This means that the following model can be seen as a development of the model seen in Figure 9.2, described previously.

Accordingly, it was important to consider a 3D case for the studied structure, to reach a strut and tie model with a good correlation to the reality. The factor, in this case, turning the structure into a 3D problem, was the steel component KBA-5, since the thickness of the component was smaller than the thickness of the concrete slab. Due to this, the load must deviate inwards to make it possible for the load to enter the steel component, see the cross-section in Figure 9.4. The plane section of the model, seen in Figure 9.4, is identical to the model in Figure 9.2. The only difference are the nodal numbers which were inserted to help the understanding of the force paths of the cross section.

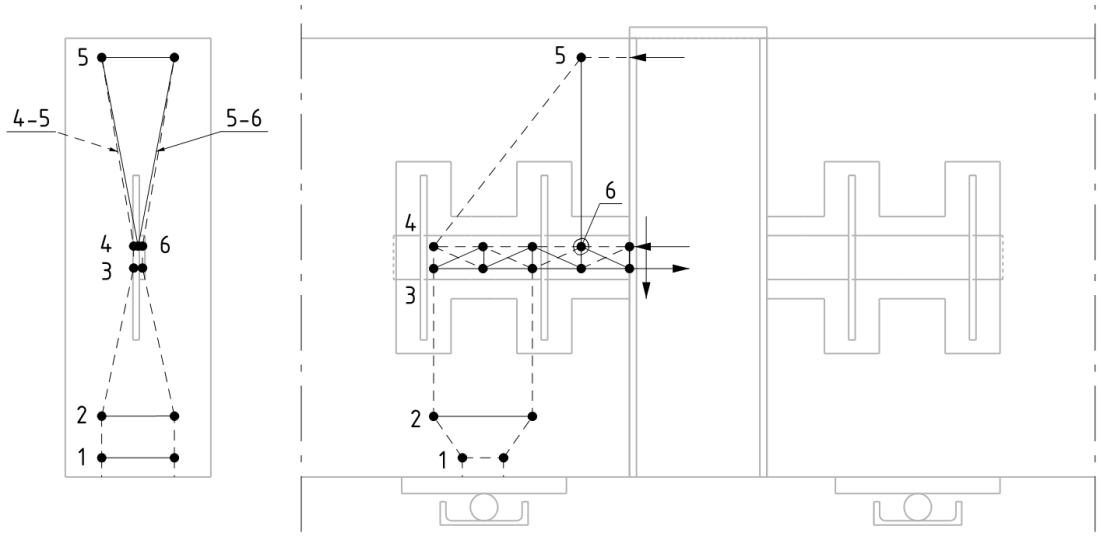

Figure 9.4 A strut and tie model of a three-dimensional case, where the hollow core units were seen as solid slabs. Nodal numbers were inserted, to help the understanding of the three-dimensional behaviour.

9.1.3 Hollow core units in 3D

In the previously described strut and tie models, the concrete members were considered as solid slabs. However, when considering the concrete members as HC units, there were additional factors, in the analytical model, which had to be considered.

As mentioned in Chapter 2.1, HC units carry in-plane forces differently in different directions. This makes an analytical model of the studied connection even more complex than the previously described models, since the load paths must be considered differently. When performing calculations of the load paths between two nodes for HC units, the loads are thus transferred either through the webs or the flanges. However, it is important to have in mind that loads always aim for transmission through materials of the greatest stiffness and takes the shortest path possible. As the recess of the HC units, where the steel component KBA-5 was located in, was filled with grout, the recess turned into a solid concrete element. The stiffness of this solid concrete part was thus of higher stiffness than the stiffness of the flanges of the HC unit, which, in turn, compelled the forces to be transmitted through the grout instead of the flanges.

In the analytical model presented in Figure 9.5, the fourth node was vertically located closer to the steel component, than its corresponding nodes were in the other models. This since the load was presumed to be transferred through the grout, as described previously. Altogether, the model presented in Figure 9.5 was similar to the previous ones described, except for the load transmission below the steel component KBA-5, due to the load transferring properties of the HC units. In contrast to the previous analytical models, the loads deviated from the supports into two different load paths below the steel component; this model only presents one load path, in 2D, between the steel component KBA-5 and the supports. This is since the HC units only can transfer loads in the y-direction through the webs.

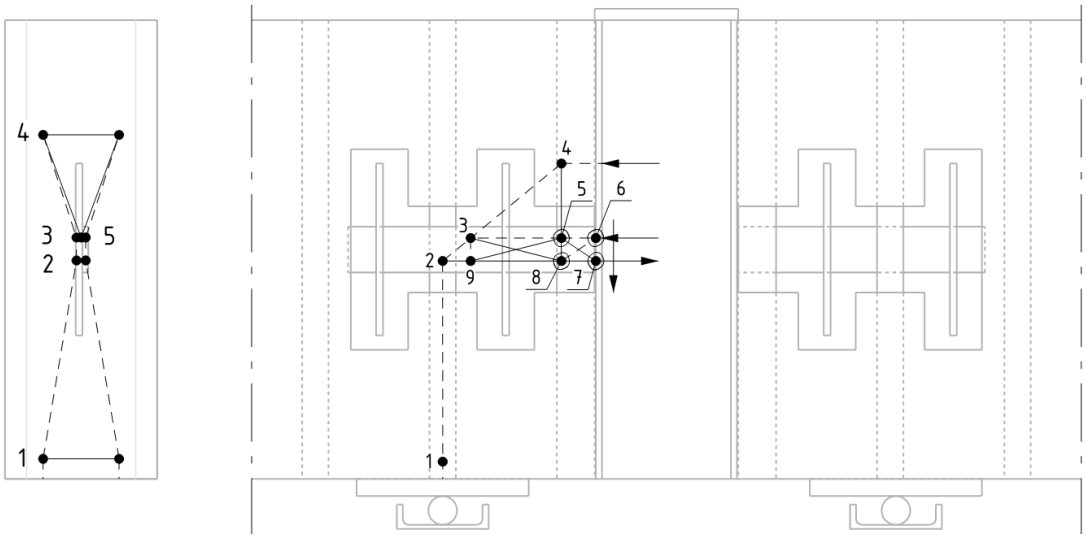

Figure 9.5 A strut and tie model in three dimensions, of the studied case. The compressive forces were transferred from the grout, through inclined struts, to the steel component KBA-5. The compressive forces were then transferred from the steel component, to the support, through the web.

As in the first case described, the model according to Figure 9.1, the plastic sheet in the joint between the HC units and the steel beam, was considered to reduce all the force transfer through friction in the joint.

Regarding the most critical parts of the concrete members in this design, and that concrete is a tensile tender material, it was found that the path between node 4 and 5 needed caution, alternatively also tensile forces at node 7 as large tensile forces were to expect at this location.

Finally, this model was assumed to be a reasonable model representing the structural test and is further referred to as the final analytical model. It includes essential factors, such as the cross-section of the HC units and the differences in stiffness of the grout and the concrete of the HC units, into account. Therefore, only calculations of this model were performed in Chapter 10.

9.2 Longitudinal edge joint

Equation (5.1), regarding longitudinal end joints, requires an external normal force perpendicular to the joint, to be valid. In the designed test arrangement, the components were placed next to each other and no initial external normal force was applied. Though, the steel component KBA-5 generates a normal force on the test arrangement when it is loaded. In other words, the component has to be "activated" before the test specimen is subjected to any kind of normal forces perpendicular to the joint. The normal force which should be used in the equation was thus complicated to predict, due to the need of activation and that it would increase as the appliance of load increased. To find a capacity, which was dependent on the load application, further investigations were required and will not be a part of this study and thus, this equation was found not to be useful.

Of course, an initial, controlled compressive force surrounding the test specimen, could have been applied when the structural tests were performed to achieve the needed conditions for this equation. This would though not reflect a real case in a prefabricated

structure, since there are no compressive forces keeping the floor structure and an outer steel beam together.

10 Results and Analysis from Analytical Model

In this Chapter, results from the calculations of the final analytical model, described in Chapter 9.1.3, are presented. First, the model is controlled for equilibrium, to achieve load-carrying relations, further called unit loads, between the struts and ties. Further, capacities of parts found most vital are calculated and assumptions made during the procedure are explained. Finally, the final analytical model is compared to the results from the structural tests, based on the expected failure load and final crack pattern, to find out if the analytical model reflected the structural behaviour of the test specimen.

10.1 Equilibrium and unit loads

The following Sub-chapters first present the procedure of modelling the final analytical strut and tie model in 2D. This was done to simplify the understanding of the following 3D-model, which was used to achieve the unit loads and the final expected failure load for vital elements of the final analytical model.

In the final model, which can be seen in Figure 9.5, some nodes were statically indeterminate. Thus, an estimation of how much of the applied load, each strut and tie would carry in the final analytical model, had to be made. As the total applied load must be transferred to the support at the second web, the strut towards the support was the only, in advance known, unit load. This was an input for the final analytical model when modelling it in both 2D and 3D. Subsequently, the unit loads for the remaining struts and ties originated from the mentioned strut. In turn, the unit loads for the vital elements, were achieved.

10.1.1 2D-model in pointsketch2D

To model the final analytical model in 2D, the software programme pointSketch2D, which is aimed to increase the understanding of 2D trusses, was used. The struts, ties and reaction forces modelled in the final analytical model are further called elements, and in pointSketch2D, the elements have no specific material properties, as stiffness etc. All nodes, marked with yellow colour, struts and ties were modelled in this programme, together with different BC's of the outer nodes, see Figure 10.1.

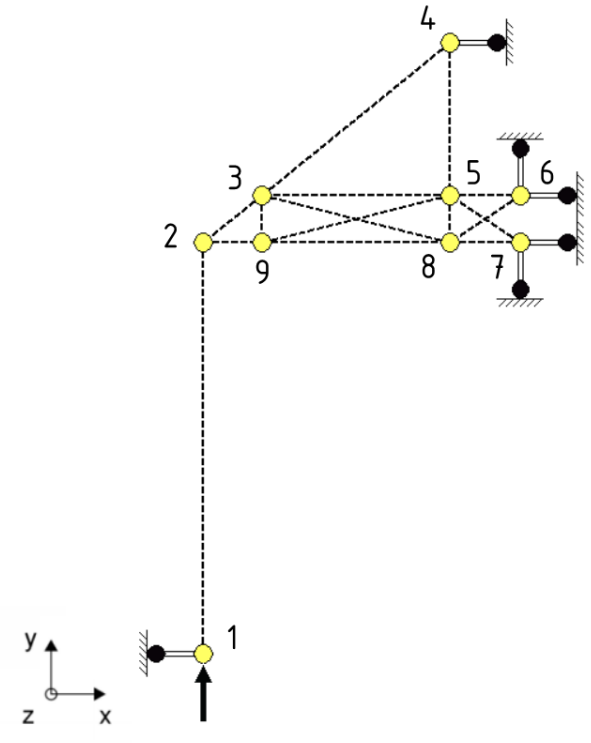

Figure 10.1 The final analytical model with nodal numbers, modelled in the software programme pointSketch2D. Node 1 and 4 were supported in the x-direction, while node 6 and 7 were supported in both x- and y-direction. In node 1, an applied unit load, with a magnitude of 1, was inserted in the y-direction.

To create global equilibrium in the modelling programme, node 1, the location of the support reaction, was locked in the x-direction. The arrow in Figure 10.1, representing the support reaction, was set to 1, as this was the force which corresponded to the, in advance known, unit load. The main difficulty with the final analytical model was to estimate the forces between the HC units and the steel beam. In other words, there were uncertainties about the magnitude of forces transferred through the steel component KBA-5, at node 6 and 7, compared to forces transmitted between the concrete and the steel beam in node 4. As the latter node was prevented to move in the x-direction, a support, in the model of pointsketch2D, was added in that direction. Node 6 and 7 were located in the joint between the steel beam and the component KBA-5, and were thus prevented to move in these directions, x- and y-direction. Thus, supports were added in those directions for node 6 and 7. By this, it could be seen that a global equilibrium was achieved. The results can be seen in Figure 10.2.

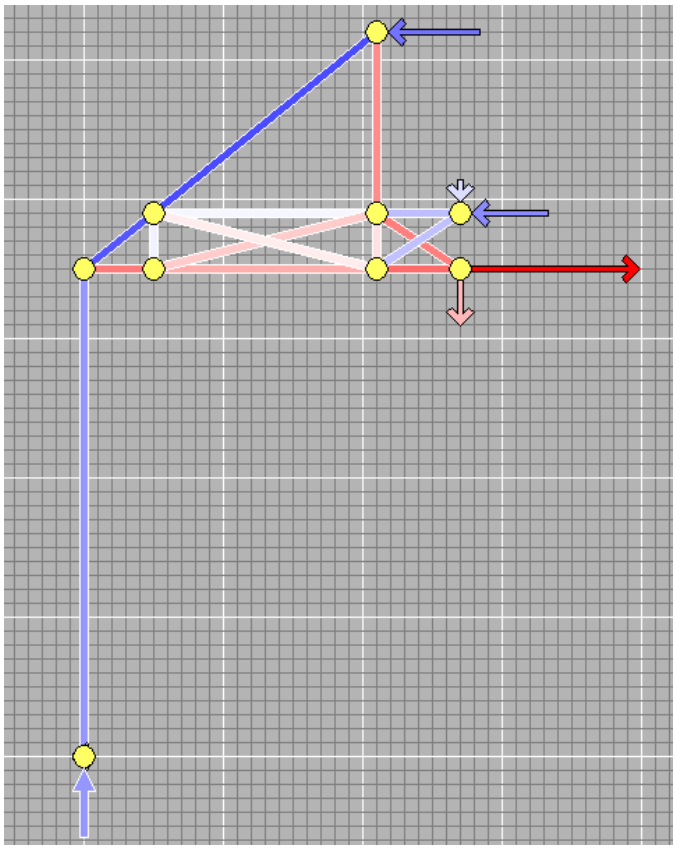

Figure 10.2 The results from pointSketch2D, showing compressive and tensile forces. The blue colour shows compression and red colour shows tension, the larger opacity – the higher unit load in the specific element.

10.1.2 3D-model SAP2000

As mentioned in Chapter 9.1, the studied connection was a 3D problem. Neglecting and simplifying such a system into a 2D problem was not preferred as the actual complexity of the structure would then be neglected.

To analyse the final analytical model in 3D, the software program SAP2000, which is a software for analysis and design of structural systems, was used. In the software, the elements were assigned to material properties, to the same material properties as in pointSketch2D. In other words, the effect of gravity and stiffness of the different materials was not considered in the calculations of SAP2000.

When the model was considered in 3D, some elements were inclined and divided into two components. This, in turn, added more nodes to the model, as can be seen in Figure 10.3. In the model, the number of nodes inside the steel component KBA-5 were simplified to be only one in the z-direction, in other words, in the cross-sectional view of the steel component. In Figure 10.3, the final analytical model is placed inside one side of the test setup, to simplify the understanding of how the analytical model was acting in three dimensions.

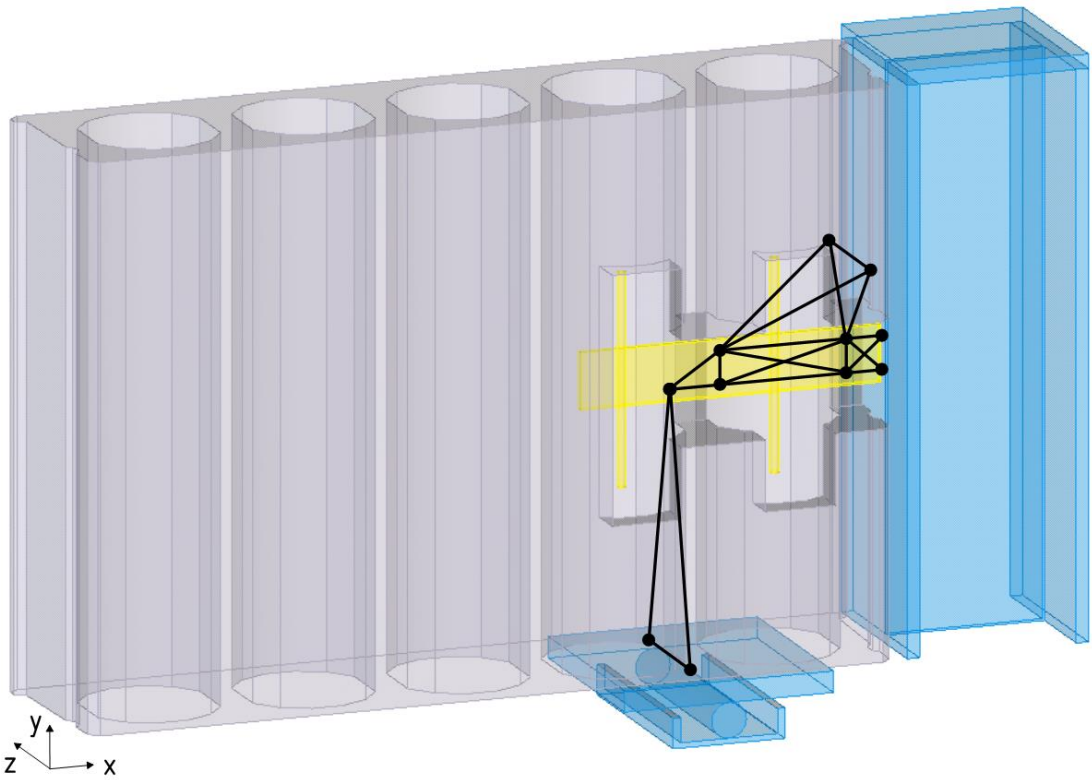

Figure 10.3 The final analytical model in 3D, inside one side of the test setup.

The BC's used for the 2D modelling in pointSketch2D was an input in SAP2000 too, together with suitable BC's in the third dimension. As can be seen in Figure 10.4, the nodes earlier representing node 1 and 4, were now divided into two different nodes, each. The nodes, 1A, 1B, 4A and 4B were prevented to move only in the x-direction. By this, the presumed tensile forces represented by element 22 and 23, between the A- and B-nodes, were allowed to occur. Further, the nodes inside the steel component KBA-5 (node 2, 3, 5, 8 and 9 in Figure 10.1) were prevented to move in the z-direction since it was presumed that such a movement was expected to be small and not have a large impact of the results. Node 6 and 7 (in Figure 10.1) were fully restrained, thus no movements in any directions were allowed to occur.

As the total applied load was presumed to enter the supports vertically at node 1A and 1B, a vertical point load in those nodes were assigned. The two point loads had the magnitude of 0.5 each, in order to together represent the total applied unit load (equal to 1 in the 2D-model), and thus the in advance known unit load. The most vital elements were considered to be all the elements acting in the concrete parts (element 1-1, 1-2 14-1, 14-2, 15-1, 15-2, 22 and 23) and the reaction forces, in the x-direction, at node 4A and 4B (element 21A and 21B). Also, the elements located in the lower part of the steel component KBA-5 (element 2, 3 and 4) and the reaction force, in the x-direction, at node 7AB (element 18), were vital due to large tensile forces. The latter elements were chosen to see if, and where, the steel component KBA-5 reached yielding. The most vital elements and nodes where the most vital reaction forces were acting, can be seen in Figure 10.4.

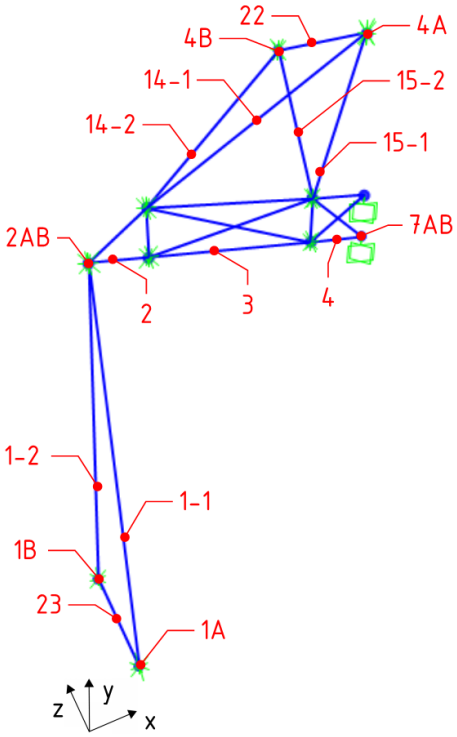

Figure 10.4 The final analytical model in 3D, modelled in SAP2000. Numbers and letters represents the most vital elements and the nodes where the most vital reaction forces were acting.

The tensile and compressive forces, due to the applied unit loads and BC's, in each element can be seen in Figure 10.5.

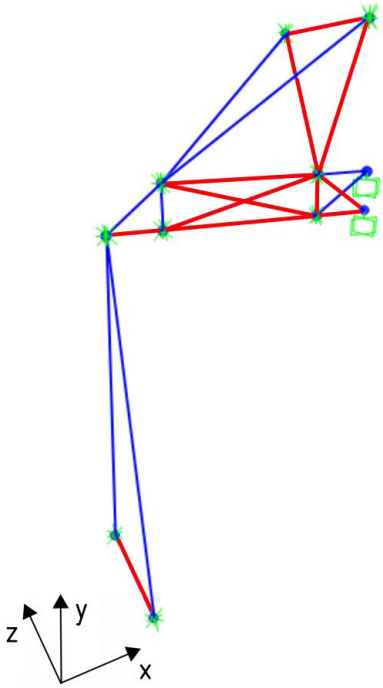

Figure 10.5 The results from SAP2000, showing in which element tensile or compressive forces were acting. The blue colour shows compression and red colour shows tension. It should be noted that the opacity of the colours do not reflect the magnitude of the unit loads.

The unit loads achieved from SAP2000, for the most vital elements, can be seen in Table 10.1.

Table 10.1 The unit loads, from SAP2000, of elements that were found to be vital for the load-carrying capacity. Some elements had two components when studying the model in 3D and were therefore divided into two. The material they were affecting, can also be seen. Negative values of the unit loads represent compressive forces, while positive values represent tensile forces.

Element	Material	Unit loads
1-1	HC unit	-0.5054
1-2	HC unit	-0.5054
14-1	Grout	-0.3139
14-2	Grout	-0.3139
15-1	HC unit	0.2228
15-2	HC unit	0.2228
21-A	HC unit	-0.2517
21-B	HC unit	-0.2517
22	HC unit	0.0048
23	HC unit	0.0754
18	KBA-5	0.6523
2	KBA-5	0.2850
3	KBA-5	0.1421
4	KBA-5	0.3304

10.2 Load capacities of elements

To determine the load capacities of the elements, the cross-sectional areas that contributed to the load-carrying capacities needed to be estimated. The elements located in the webs of the HC units, element 1-1, 1-2, 15-1, 15-2, 22 and 23 were assumed to have a contributing width equal to one web thickness, 35 mm, thus it was assumed that the full width of the webs could carry the load. Regarding the choice of width for element 14-1 and 14-2, inclined struts inside the grout, it was found appropriate to set the width to twice the thickness of one web, 70 mm, as it was assumed that the loads possibly would deviate into a larger area at this location. The width for element 21-A and 21-B, acting in the x-direction in node 4A and 4B respectively, was set to 70 mm, corresponding to twice the size of one web, as for element 14-1 and 14-2.

For all inclined elements located in the concrete parts, it was found appropriate to assume a contributing height of 25 % of the total height of the test specimen, 265 mm, not to overestimate the capacity. In other words, each inclined element was acting in the half of the height of the test specimen and it was presumed that the load could only deviate into 50 % of the half height of the test specimen (25% of the total height = 66.25 mm). Regarding the compressive reaction forces, element 21-A and 21-B, the same assumption was made, thus their height was set to 25 % of the total height of the test specimen. For the ties, elements 22 and 23, their assumed contributing lengths were set to 35 mm, equal to the thickness of one web. Further, it was assumed that the loads could only spread over a length equal to a size of two webs, 70 mm. It should though be noted that the total length of the test specimen was 800 mm. However, it was found not to be reasonable to assume such a load distribution, as the load is only transferred between node 1A and 1B and that loads always takes the shortest path. The contributing areas were further multiplied by the related average (compressive or tensile) strengths, depending on what type of force was acting in each element, to achieve a capacity.

The steel wires located in the first web, closest to the steel beam, could be presumed to have contributed to the capacity of element 15-1 and 15-2. However, the effect from the steel wires were neglected, as the anchorage length was assumed to be too small, due to the length of the HC units.

The capacity of the steel component KBA-5 was calculated based on the yield strength of the component since it was of interest to know when the component started to plastically deform. The forces transmitted through the steel plate, were assumed to act along the full thickness of the plate, 10 mm, and only 75 % of the total width, 80 mm, was utilized for tensile forces. In other words, it was assumed that 25 % of the width of the plate was subjected to compressive forces. The capacities of each element are presented in Table 10.2.

Table 10.2 The capacities of the elements that were found vital for the load-carrying capacity, and which material the element was located in. The dimensions of the width and height/thickness/length used for the contributing area, the average, compressive or tensile, strengths for the concrete and the yield strength for the steel component KBA-5 can also be seen. Negative values represent compressive load capacities, and positive values represents tensile load capacities.

Element	Contributing width [mm]	Contributing height/thickness/length [mm]	Average strength [MPa]	Load capacity [kN]	Material
1-1	35	66.25	50.3	-116.6	HC unit
1-2	35	66.25	50.3	-116.6	HC unit
2	60	10	355	213	KBA-5
3	60	10	355	213	KBA-5
4	60	10	355	213	KBA-5
14-1	70	66.25	37.2	-172.5	Grout
14-2	70	66.25	37.2	-172.5	Grout
15-1	35	66.25	3.6	8.3	HC unit
15-2	35	66.25	3.6	8.3	HC unit
18	60	10	355	213	KBA-5
21-A	70	66.25	50.3	-233.3	HC unit
21-B	70	66.25	50.3	-233.3	HC unit
22	35	35	3.6	4.4	HC unit
23	35	35	3.6	4.4	HC unit

As can be seen in Table 10.2, the capacities for element 15-1, 15-2, 22 and 23 were lower than the other capacities. This is due to that these elements were the ones, inside the concrete parts, that carried tensile forces, as can be seen in Figure 10.5. In Table 10.2, it can also be seen that the capacity of each element inside the steel component KBA-5 had equal capacity, this since the capacity was calculated based on the same contributing area and the same yield strength.

10.3 Expected failure load

It was found that the final expected failure load of the analytical model was reached when redistribution of forces within the concrete could not continue. When studying the final analytical model, possible ways of redistributing of forces could be found and the model could be thought of as three different parts. One part constitutes of elements

located inside the steel component KBA-5, in other words the vital elements 2, 3, and 4. The elements located in the concrete could be thought of as two parts; one above the steel component (element 14-1, 14-2, 15-1, 15-2 and 22) and one beneath the steel component (element 1-1, 1-2 and 23). The part above the steel component, is statically indeterminate which means that a failure of this part would redistribute its forces to the steel component, thus expose KBA-5 to larger forces. In other words, a failure of the upper part would not result in a complete failure of the analytical model. In contrast, the lower part, consisting of elements in concrete, is statically determinate and a failure in this part would cause a complete failure of the analytical model.

The expected failure load for the vital elements, were achieved by dividing each capacity from Table 10.2 by the corresponding unit loads in Table 10.1. The results regarding the expected failure load for each element, can be seen in Table 10.3. The elements marked with red colour were the ones with the lowest expected failure load, when the complete analytical model was studied.

Table 10.3 The expected failure loads of all the vital elements, where the capacities for each element were divided by each respective unit load. Which material the element was located in, is also presented. The elements marked with red colour were the ones which had the lowest expected failure load, when the complete analytical model was studied.

Element	Expected failure load [kN]	Material
1-1	230.8	HC unit
1-2	230.8	HC unit
2	747.4	KBA-5
3	1499.3	KBA-5
4	644.7	KBA-5
14-1	549.6	Grout
14-2	549.6	Grout
15-1	37.5	HC unit
15-2	37.5	HC unit
18	326.6	KBA-5
21-A	926.7	HC unit
21-B	926.7	HC unit
22	919.8	HC unit
23	58.5	HC unit

From Table 10.3, the first elements to reach failure was likely to be 15-1 and 15-2 since their expected failure loads were the lowest. But as mentioned, the part above the steel component, which element 15-1 and 15-2 was a part of, was not decisive for the load-carrying capacity of the complete analytical model. However, regarding the part above the steel component and the results in Table 10.3, one obtained failure load was unexpected. This was element 22, an element which could carry tensile forces to an approximate value of 920 kN. As the element carried tensile forces, it was presumed that the expected failure load would have been smaller, as concrete has a low tensile strength. The reasons behind this is further discussed in Chapter 11.3 and Chapter 11.4.

A complete failure was to expect when element 1-1, 1-2 or 23 reached failure. Thus, the lowest expected failure load of one of those elements in Table 10.3, would represent the final expected failure load. The expected failure loads for the decisive elements are compiled in Table 10.4, to simplify further discussion.

Table 10.4 The expected failure loads for the decisive elements in the final analytical model.

Element	Expected failure load [kN]	Material
1-1	230.8 ≈ 231	HC unit
1-2	230.8 ≈ 231	HC unit
23	58.5 ≈ 59	HC unit

As can be seen in Table 10.4, the lowest expected failure load for the decisive elements of the analytical model, could be found in element 23. In other words, the final expected failure load was approximately 59 kN.

To strengthen the argument of that the lower part was decisive regarding the expected failure load, an analytical model of this part only was performed. This was done by modelling the lower part only in SAP2000 and prevent all movements of node 2AB (in Figure 10.4). Node 2AB was prevented to move in any direction to reach global equilibrium of the simplified model. The lower part of the final analytical model can be seen in Figure 10.6.

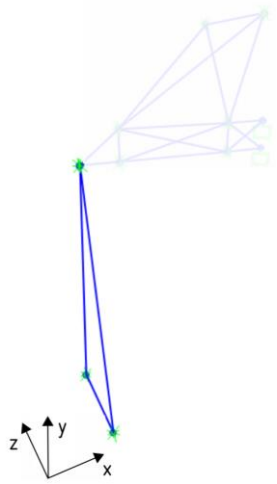

Figure 10.6 The lower part, in blue color, of the analytical model, used to strengthen the argument of decisive parts for the expected failure load.

When the lower part only was modelled, the results regarding the unit loads achieved from SAP2000, showed the same results as when the complete analytical model was modelled, thus the same unit loads as in Table 10.1 for element 1-1, 1-2 and 23. In other words, the unit loads for these elements do not change until failure in element 23 has occurred. By this, the argument was strengthened, and the final expected failure load was set to approximately 59 kN.

10.4 Comparison between analytical results and structural tests

To see how well the final analytical model corresponded to the performed structural test, the results from Chapter 10.3 were analysed based on the results from the structural tests and the final crack pattern described in Chapter 8.

It should be noted that the analytical model only reflected a statically and linear behaviour, in other words, no redistribution of the forces was reflected by the final analytical model. When the first crack appeared in the test specimen, the forces aimed to reach other parts of the structure with a higher stiffness. As other parts in the structure failed, the cracking propagated. By the knowledge gained from the analytical model, assumptions of the crack propagation could be made.

As the lowest expected failure load was found in element 15-1 and 15-2, located in the web closest to the steel beam, it could be assumed that the cracking in the structural tests started in those elements. Since both elements were subjected to tensile forces, cracks would appear perpendicular to the elements in the model. In other words, cracks perpendicular to the length of the HC unit, were to expect. This could be seen in test 2 and 3, and in test 5 a small indication of such cracking could be seen. See Figure 10.7, showing a crack formation, which likely can be related to element 15-1 and 15-2.

Figure 10.7 A crack perpendicular to the length of the hollow core unit appeared during the structural tests, likely related with the tensile forces in element 15-1 and 15-2.

A failure of element 15-1 and 15-2 implies that the remaining elements of the upper part of the analytical model must carry a larger part of the applied force, and that the steel component would be exposed to larger forces. The unit loads for the remaining elements in the upper part increases, which in turn reduces their expected failure load.

After horizontal cracking corresponding to elements 15-1 and 15-2, cracking in element 23, located in the second web of the HC unit, was to expect as the next element to fail, see Table 10.3. As mentioned previously, a failure in element 23 would mean a complete failure of the analytical model, in other words the test specimen. Cracks correlating to the mentioned element could also be found in every cross-sectional photo for the failing HC units, which can be seen in Appendix A and Figure 10.8.

However, cracks possibly corresponding to element 22, located in the first web of the HC unit, above the steel component, could also be found in the cross-sectional photos from the structural tests, see Figure 10.8. The expected failure load for element 22, seen in Table 10.3, was 920 kN, i.e. significantly higher than both the average experimental failure load and the expected failure load for element 23. Despite that, a redistribution of forces, due to failure in element 15-1 and 15-2, were to expect, and as mentioned the expected failure load for element 22 would then be reduced. The magnitude of such a reduction was difficult to estimate by the analytical model. But as cross-sectional cracks at the location of element 22 could be identified in the photos from the structural tests, it was assumed that the forces redistributed in a way that caused failure of the element, regardless the expected failure load from the statically and linear analytical model for the element. Further discussions regarding the obtained expected failure load of element 22 is presented in Chapter 11.3 and Chapter 11.4.

One argument strengthening the hypothesis that the cracks in the cross-sectional photos were assumed to correspond to element 22 and 23, was also the direction of the cracks. As for element 15-1 and 15-2, the cracks appeared perpendicular to the first and second web, perpendicular to the direction of the elements. The reason why the crack corresponding to element 23 was located closer to the lower flange of the HC units, was assumed to be due to propagation through the joint between the grout and the HC unit, as described in Chapter 8.

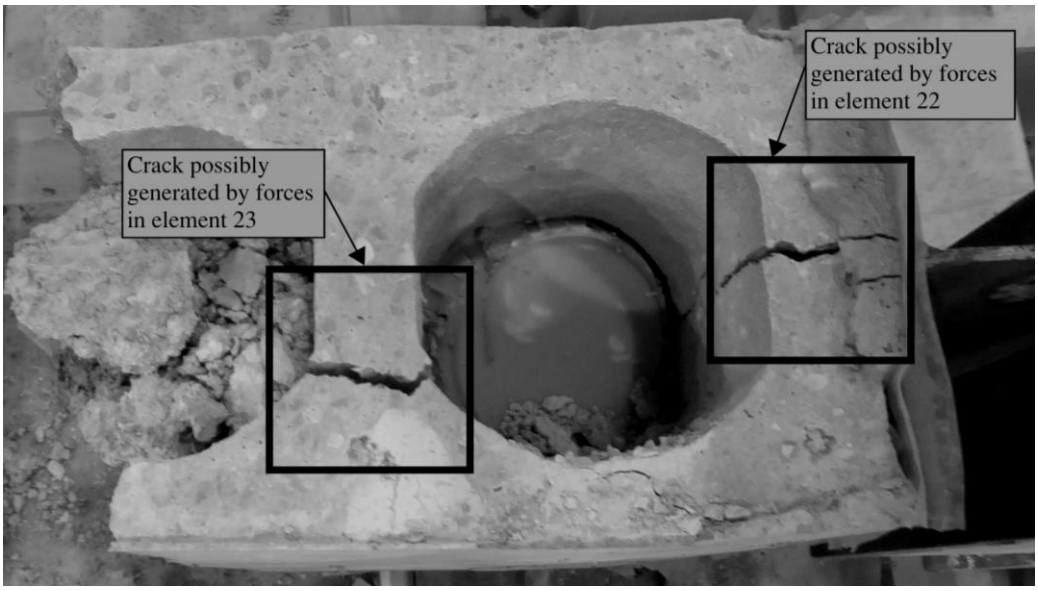

Figure 10.8 Cracks perpendicular to the webs appeared during the structural tests, possibly coming from the tensile forces in element 22 and 23.

From Table 10.3, it could be seen that element 18, transmitting forces between the steel beam and the steel component KBA-5, had an expected failure load of approximately 327 kN, which was higher than the average experimental failure load, 200 kN. Thus, according to the analytical model, the steel component would not have started to yield for the average experimental failure load. However, from the photos of the two steel components which were taken out of the HC units, yielding could be seen at the location of element 18, see Figure 10.9. This was also assumed to be due to redistribution of forces when the elements in the concrete cracked, which in turn probably mean an increase of the unit loads in the steel component, as mentioned previously.

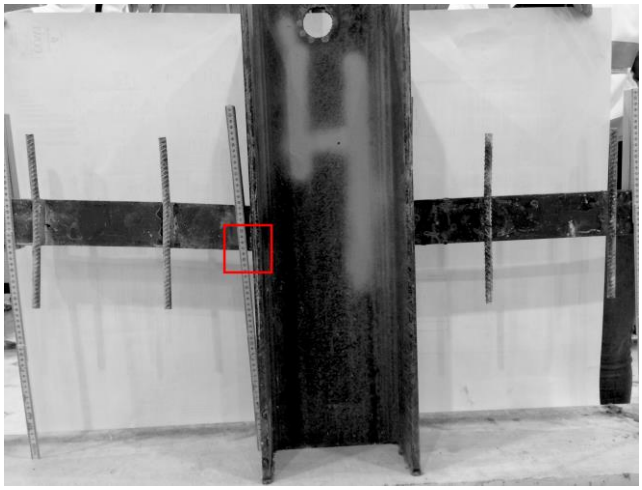

Figure 10.9 Yielding of the steel component KBA-5 appeared during the structural tests, possibly generated by tensile forces from the reaction force, element 18, between the steel beam and the steel component KBA-5.

From Table 10.4, the final expected failure load for the final analytical model was 59 kN, corresponding to element 23. This load approximately represents 30 % of the average experimental failure load, 200 kN. Since the final analytical model was based on the strut and tie method, a lower bound approach, the values from the analytical model should be on the safe side compared to structural tests. As the final expected

failure load was lower than the average experimental failure load, it could be presumed that the analytical model reflected the structural behaviour of the performed structural tests in a good manner. Further, there was a reasonable correlation between the failing elements and the crack patterns obtained in the structural tests.

11 Discussion

In this Chapter a discussion regarding the gained knowledge from the literature study, the structural tests, the analytical model and the final analytical model, is carried out.

11.1 Test setup

As the material concrete requires time to cure, and a test with a final concrete strength was desired to be performed, the planning of how to assemble the test arrangement was done under a limited period of time. The required 28 days of the grout to cure, in combination with that it would be time left to complete the report of the study, gave a restricted amount of time for the planning. Subsequently, it was assumed that performance of a finite element analysis (FEA), of both the designed test arrangement and a larger floor structure, would have been advantageously. By such an analysis, possible differences in behaviour between a real structure and the test set up could have been discovered and thus avoided. In other words, possible improvements of the test arrangement could have been achieved if the study was performed during a greater period of time, and if a FEA would have been performed as a starting point of the study.

The real structural behaviour of a floor system is rather complex since the response depends on several individual elements tied together. In other words, the loads affecting the studied connection in a real structure, are coming from all HC units of the floor system, and thus not only the HC unit the connection is located in. Due to the limitations of the test machine, such a behaviour would not be possible to achieve. Instead the forces within the test specimen were more concentrated, than in a real structure. It could be stated that both the load application and the support conditions would expose the test specimen to high concentrated forces, which probably do not occur in a real structure. On the other hand, this could be seen as a "worst case" of a real structure, although it is very unlikely that it would occur. However, HC units are, theoretically, supported along the full width at the short edges in a real structure. As the surfaces of the HC units have a certain roughness and irregularities, the behaviour of a fully supported short edge is difficult to achieve. In other words, a support condition as the ones in the performed structural tests in this study, cylinders creating concentrated stress fields, could possibly be the case in a real structure, but definitely not with the same magnitude.

11.2 Structural tests

To study the effect of the concentrated stress fields, two support locations (second or fourth web) were tested. When the results were analysed, it was realised that the support location at the second web reflected the real behaviour better, as it limited the rotation. A rotation of the complete floor structure is unlikely to occur, due to the in-plane rotational stiffness of a full working floor structure.

When performing the structural tests, three main results were obtained. These were the experimental failure loads, final crack pattern and films from one side of the test arrangement. A load-deflection curve of the structural tests could have been helpful during the analysis of the results from the analytical model. This since a comparison between the simulation of the force redistribution in the analytical model and the load-deflection curve could have been carried out. A desired load-deflection curve was

though not achieved in this study as it was difficult to guarantee the correlation between the measurement devices and the load application, as described in Chapter 7.2. On the other hand, the aim of the study was to estimate the maximum load carrying capacity of the studied connection, although, as mentioned, it would have helped the understanding of the structural behaviour and the crack propagation of the tests.

The two sizes of the HC units - half and full width - were tested to see if the outer end of the HC units did affect the results, as it statically was presumed not to be the case from the beginning of the study. From the results, the two sizes with the same support location, tests 2, 3 and 4, 5 gave different results regarding the final crack patterns. It could on films for the mentioned tests, be noted that an outward rotation occurred for tests 4 and 5, after the first crack and loss of stiffness. This was due the larger part of the HC unit outside the support. Since such a rotation usually is not the case in a real structure, the differences in behaviour during the tests were assumed to be due to the designed test setup. If a fully supported short edge instead would have been reflected for tests 2, 3, 4 and 5, it was likely that the same final crack patterns could have been achieved. However, the experimental failure loads for the tests of HC units with different sizes showed similar values. This in turn indicate that the outer part of the HC units did not affect the load-carrying capacity and the assumption was confirmed.

The timber planks that were put up to ensure safety during the tests, seemed to affect the results of tests 4 and 5, regarding the crack propagation, if the films from the tests were studied closely. As mentioned, the vertical cracks propagated from two different directions, from the bottom and the top respectively. However, regarding the experimental failure loads, seen in Table 8.1, there were no significant difference between the two tests. Altogether, it was difficult to determine if the timber planks affected the crack formations only, or if they also affected the experimental failure loads.

11.3 Final analytical model

According to Engström (2015), a strut and tie model is normally used to design discontinuity regions in order to discover the need of reinforcement, where the ties are located. Furthermore, it can be several strut and tie models representing the same problem. In this study, the strut and tie method was mainly used to estimate the structural behaviour and the flow of forces in the test arrangement. In other words, the final analytical model presented in this study, was one proposal of how the structural behaviour of the test arrangement could be reflected. It should therefore be noted that the structural behaviour of the studied test arrangement could have been reflected by several other strut and tie models and that the final model possibly could be optimized.

Node 4 in the final analytical strut and tie model was located at its position to create an inclined load path through the grout in the recess since this was the presumed load path during the structural tests. However, this location could have been different, which in turn would have resulted in other unit loads from SAP2000, for the elements in the analytical model. If the node would have been located closer to the steel component KBA-5 in the y-direction, the unit loads in the elements above the steel component would have decreased. This, in turn, exposes the steel component to larger forces. In the opposite, the forces acting in the steel component could have been reduced by moving the fourth node upwards, away from the steel component. This possibly would have resulted in an additional load deviation of element 14-1 and 14-2, as the load-

carrying properties of the HC units would have had to be considered more carefully. Therefore, it was found that the fourth node in this study was properly located.

When modelling the final analytical model in SAP2000, the elements were modelled to carry loads equally. Of course, this was a simplification as struts and ties in real structures carry loads differently, as they possess different stiffness properties. In other words, compressive struts in concrete are able to carry a larger part of the loads acting in the structure, compared to ties. It should also be noted that the analytical model developed in this study, aimed to reflect a complex strut and tie model based on the test arrangement, and that simplifications needed to be done.

As element 22 was a tie inside the HC unit, subjected to tensile forces, and that ties in concrete parts are able to carry less forces than struts, the achieved expected failure load for element 22, 920 kN, was found to be unreasonable. It was presumed that the expected failure load for this element should have been lower as it carried tensile forces. However, the unit load for the mentioned element from the analytical model, was significantly lower than for the rest of the vital elements. In other words, the element 22 did not carry a large part of the applied load, and a high expected failure load was therefore obtained. The contradiction between what was expected on beforehand (low failure load) and the obtained expected failure load from the analytical model (high failure load), was presumed to reflect inaccuracies in the upper part, above the steel component, in the analytical model. Why these inaccuracies were presumed is further discussed in the following chapter, Chapter 11.4.

11.4 Comparison between analytical results and structural tests

As the results from the analytical model was compared to the results from the structural tests, additional reasons for the crack pattern, were observed. One example was the cracks in the cross-section, perpendicular to the first and second web. Firstly, only based on the final crack pattern from the structural tests, it was assumed that the cracking was due to high stresses in the steel component KBA-5, and that a knife-like behaviour from the component was the reason behind the cracking. As the analytical model also considers the behaviour of the steel component, the ties, element 22 and 23, also originated from stresses inside the component, it was presumed that the analytical model convincingly described the influence from the steel component KBA-5. In other words, the analytical model corresponded well to the structural tests.

The doubts about the upper part of the analytical model, which was presumed to give an unreasonable expected failure load for element 22, were confirmed by the results from the structural tests. This since cracks possibly corresponding to element 22 were, as mentioned, found in all the cross-sectional photos. It was thus presumed that the elements in the upper part of the analytical model had too low unit loads, which in turn resulted in too high expected failure loads, compared to what occurred in the structural tests; especially for element 22. The reasons for this were presumed to be due to the neglected differences in stiffness of the struts and ties, located in different materials. Another reason which also could explain the differences, could be possible, additional forces due to friction between the steel beam and the HC units. These were, as mentioned, neglected in the analytical model, as plastic sheets, aimed to reduce such contribution, were added in the test setups. It is though difficult, as mentioned, to reduce forces due to friction in practice. To take the additional forces due to friction into

account in the analytical model, forces should possibly have been added in the y-direction in node 4A and 4B. However, the magnitude of such forces is difficult to determine.

As mentioned in Chapter 10.2, the steel wires in the HC units were neglected when the capacity for element 15-1 and 15-2 was calculated, since the anchorage length in the structural tests was assumed to be too small. If the wires would have been included, a higher tensile capacity in element 15-1 and 15-2 would have been achieved. This would have prevented these elements to reach failure first. The element to reach failure first, would probably instead have been element 23. It should be noted though, that elements 15-1 and 15-2 were inclined, while the wires are placed in bottom and along the length of the HC units. By this, it could be assumed that the wires would not help element 15-1 and 15-2 to carry tensile forces, at least not to the maximum capacity of the wires. Therefore, neglecting the wires capacity was found to be a reasonable assumption, as a result on the safe side was obtained.

As the analytical model was based on a lower bound approach as the strut and tie method, and that the final expected failure load was estimated to 59 kN which only corresponded to 30 % of the average experimental failure load; the analytical model was found to correspond reasonably well to the structural tests performed in this study. This as a result on the safe side was to expect, when utilizing such a method.

12 Conclusions

From this work, the following conclusions could be drawn:

- From the literature study, it was found that the critical part in a floor system, is at the longitudinal edge of the outermost HC unit, as the forces are transmitted to this section from the neighbouring floor units. In other words, this is where the maximum shear force is found.
- In the structural tests, the length of the HC units was 800 mm. In a real structure, the units are longer, and more connections are added into the units. Thus, the connection in the structural tests, was subjected to concentrated loads, in contrast to reality where it is subjected to evenly distributed shear forces along the HC unit. Thus, the used test arrangement does not reflect a real structural behaviour of the studied connection.
- From the structural tests, the maximum capacity of the designed test arrangement, could be measured. The average experimental failure load was 200 kN, for supports at second web, and 95 kN for supports at fourth web. Regarding the structural behaviour, similarities in final crack pattern could be seen for the tests with supports at the second web, for the two respective widths, half and full width of the HC units. In contrast, there were no similarities in crack pattern for the tests of full width HC units and support at the fourth web, due to different failure modes.
- The final analytical model, a 3D strut and tie model, showed good correlation with the structural behaviour of the performed structural tests, through a similar behaviour as certain, final crack patterns from the structural tests. The expected failure load from the final analytical model was 59 kN, which corresponded to 30 % of the average experimental failure load. This was found as a satisfying result, as the strut and tie method is a lower bound approach.

As a final conclusion of the study; the structural behaviour of the specific connection when loaded as in the designed test setup was reasonably well understood. However, based on the structural tests performed in this study, it was difficult to determine the structural behaviour and the load-carrying capacity of the connection including the component KBA-5, in a complete structure. Nevertheless, the structural behaviour of the studied test arrangement could be understood by using the final analytical model.

13 Suggestions for Further Studies

As mentioned, there were uncertainties of how well the structural tests in this study reflected the structural behaviour in a real structure. The main uncertainty is because concentrated stress fields were generated by the designed test arrangement. To perform a structural test that would have taken the shear forces from surrounding HC units into account, it would have been advantageous to use another type of test machine than the one used in this study.

A possible solution could be to use longer test specimens, e.g. with a length of 5 m, and place reinforcement and a layer of thick grout around the test specimen, to tie the system together as in a real structure. The test specimen should preferably also be placed horizontally, in contrast to how the tests were performed in this study. The load should be applied as it was done in this study; at one end of the steel beam, but the supports should be placed at the outer edges of the HC units, to reflect the shear forces coming from the surrounding HC units in a real structure, see Figure 13.1. This solution was discussed during the study, but the limitations of the test machine made such an arrangement impossible in the current work.

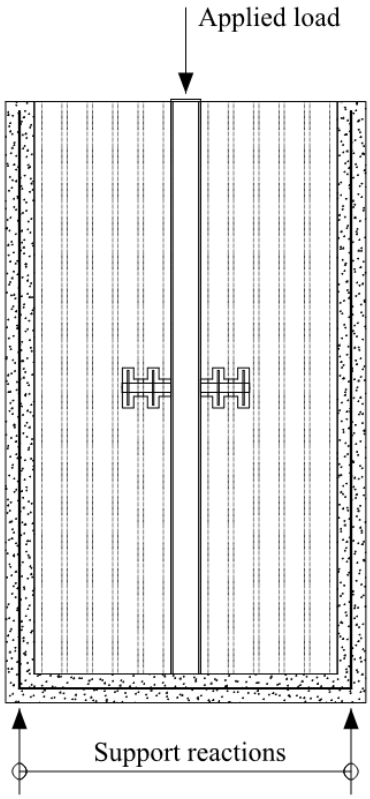

Figure 13.1 Possible test arrangement, considered to take the internal shear forces into account through the reinforcement and grout surrounding the hollow core units and the steel beam.

14 References

Al-emrani, M., Engström, B., Johansson, M., & Johansson, P. (2013). *Bärande konstruktioner*. Chalmers Tekniska Högskola, Göteborg.

Betongelementforeningen. (2013). *Betongelementboken, Bind A-H*. Oslo.

Bickley, J., & Engineers, C. (1986). Pullout testing of concrete. *Concrete Construction*. Retrieved from http://www.concreteconstruction.net/images/Pullout Testing of Concrete_tcm45-340879.pdf

Bouchair, A., Bujnak, J., Duratna, P., & Lachal, A. (2012). Modeling of the steel-concrete push-out test. *Procedia Engineering*, *40*, 102–107. https://doi.org/10.1016/j.proeng.2012.07.063

de Reese, J., Lenz, P., Zilch, K., & Plank, J. (2013). Influence of type of superplasticizer and cement composition on the adhesive bonding between aged and fresh concrete. *Construction and Building Materials*, *48*, 717–724. https://doi.org/10.1016/J.CONBUILDMAT.2013.07.054

Elliot, K. S. (2002). *Precast Concrete Structures* (First edit). Butterworth-Heinemann.

Elliott, K. S. (2000). Research and development in precast concrete framed structures. *Progress in Structural Engineering and Materials*, *2*(4), 405–428. https://doi.org/10.1002/pse.65

Elliott, K. S., & Jolly, C. (2013). *Multi-Storey Precast Concrete Framed Structures* (2nd ed.). John Wiley & Sons, Incorporated.

Engström, B. (1983). Kraftöverförande anslutningar mellan betongelement, *83*(2), 26.

Engström, B. (2015). *Design and analysis of deep beams, plates and other discontinuity regions*. Chalmers Tekniska Högskola, Göteborg.

Fib, I. F. for S. C. (2000). *Special design considerations for precast prestressed hollow core floors*. Lausanne: The International Federation for Structural Concrete.

Fib, I. F. for S. C. (2008). *Structural connections for precast concrete buildings*. Lausanne: The International Federation for Structural Concrete.

Fib, I. F. for S. C. (2013). *Model code for concrete structures* (First). Lausanne: Ernst & Sohn GmbH &Co.

Fib, I. F. for S. C. (2014). *Planning and design handbook on precast building structures*. Lausanne.

Fib Working Party 1.1.3, I. F. for S. C. (2011). *Design examples for strut-and-tie models*. Lausanne.

Kynningsrud. (2018). Om oss - Kynningsrud Prefab. Retrieved January 26, 2018, from https://www.kynningsrud.se/affarsomraden/prefab/om-prefabse/

Micallef, K., Sagaseta, J., Fernández Ruiz, M., & Muttoni, A. (2014). Assessing punching shear failure in reinforced concrete flat slabs subjected to localised impact loading. *International Journal of Impact Engineering*, *71*, 17–33. https://doi.org/10.1016/J.IJIMPENG.2014.04.003

Naderi, M. (2009). Analysis of the Slant Shear Test. *Journal of Adhesion Science and Technology*, *23*(2), 229–245. https://doi.org/10.1163/156856108X369589

Naito, C., & Ren, R. (2013). An evaluation method for precast concrete diaphragm connectors based on structural testing. *PCI Journal*, (Spring), 106–118.

PCI. (1998). PCI Manual for the Design of Hollow Core Slabs. *PCI Hollow Core Slab Producers Committee*, 141. Retrieved from http://www.getcited.org/pub/102566996

Svensk Betong. (2018). Däckelement. Retrieved March 7, 2018, from

https://www.svenskbetong.se/bygga-med-betong/bygga-med-prefab/produktredovisning/komponenter-till-hus-och-anlaggning/dackelement
Swedish Standards Institute. (2008a). Eurocode 2: Design of concrete structures - Part 1-1: General rules and rules for buildings. *Eurocode SS-EN-1992-1-1*, (138227), 236.
Swedish Standards Institute. (2008b). Eurocode 3: Design of steel structures - Part 1-1: General rules and rules for buildings. *Eurocode SS-EN-1993-1-1*, (138227), 100.
Swedish Standards Institute. (2008c). Eurocode 3: Design of steel structures - Part 1-8: Design of joints. *Eurocode SS-EN-1993-1-8*, (138227), 148.
Swedish Standards Institute. (2009). Eurocode 4: Design of composite steel and concrete structures - Part 1-1: General rules and rules for buildings. *Eurocode SS-EN-1994-1-1*, (138227).

APPENDIX

Table of Contents

APPENDIX A Cross-sectional photos from all tests

Half width hollow core units with supports at the second web

Test 2 – Steel beam located in the left side of the photo

Test 3 – Steel beam located in the left side of the photo

Full width hollow core units with supports at the second web

Test 4 – Steel beam located in the right side of the photo

Test 5 – Steel beam located in the right side of the photo

Full width hollow core units with supports at the fourth web

Test 6 – Steel beam located in the right side of the photo

Test 7– Steel beam located in the right side of the photo